Deanship of Graduation Studies

Al-Quds University

Design and Simulation of a Stretchable and Reversibly Deformable MIMO Monopole Patch Antenna for UWB Applications with High Isolation

Watan Fayez Abd Al-Raheem Zafer

M.Sc. Thesis

Jerusalem – Palestine

1440/2019

Design and Simulation of a Stretchable and Reversibly Deformable MIMO Monopole Patch Antenna for UWB Applications with High Isolation

Prepared By:

Watan Fayez Abd Al-Raheem Zafer

B.Sc.: Communication Engineering, Palestine Technical University-PTUK, Palestine

Supervisor: Dr. Mohammad Kouali

A thesis Submitted in Partial Fulfillment of the Requirements for the Degree of Master of Electronic and Computer Engineering, Deanship of Graduate Studies at Al-Quds University

1440/2019

Al-Quds University

Deanship of Graduation Studies

Electronic and Computer Engineering/Faculty of Engineering

Thesis Approval

Design and Simulation of a Stretchable and Reversibly Deformable MIMO Monopole Patch Antenna for UWB Applications with High Isolation

Prepared By: Watan Fayez Zafer

Registration No.: 201512507

Supervisor: Dr. Mohammad Kouali

Master thesis submitted and accepted, Date: 5 / 8 /2019

The names and signatures of the examining committee members are as follows:

1- Head of Committee: Dr. Mohammad Kouali Signature .....
2 -Internal Examiner: Dr. Imad Alzeer Signature .....
3 -External Examiner: Dr. Atallah Balalem Signatur .....

Jerusalem – Palestine

1440/2019

Declaration:

I Certify that this thesis submitted for the Degree of Master is the result of my own research, except where otherwise acknowledged, and that this thesis (or any part of the same) has not been submitted for a higher degree to any other university or institution.

Signed by : 

Watan Zafer

Date: 5/8/2019

Dedication

I dedicate this work to my family and anyone who cares

Watan Zafer

Acknowledgement

I would like to thank everyone who has helped me in life to reach this level. At this moment, I would like to thank my lecturers in engineering college mainly my supervisor for this project Dr. Mohammad Koali, I would like to thank him for guiding through my last two semesters.

I would like to deeply thank my mother, father, husband and all of my family for their support, helping and pursuing me during my study. Finally, my experience would not have been possible without God. Thanks a lot all.

ABSTRACT

The need to produce light weight and cheap components and devices has been the driving force for macro-electronics. Electronics that can be stretched and/or conformal to curvilinear surfaces has recently attracted broad attention so some microwave components are studied in our thesis.

In this work a design of printed rectangular monopole antenna for Ultra-Wide Band (UWB) applications is presented. The printed antenna is designed by using HFSS program to achieve the best reflection coefficient. Moreover, the stretching effect on the antenna response is studied along x-axis and y-axis. Also, compact UWB Multiple-Input Multiple-Output (MIMO) antennas are designed. In order to enhance impedance matching and improve the isolation, each UWB MIMO antenna which consists of two comparable monopole elements is proposed with different slotted stubs on the ground plane. The reflection coefficient, mutual coupling, peak gain and radiation patterns are analysed.

نمذجة و محاكاة هوائي أحادي القطب متعدد المداخل و المخرجات مطاطي قابل للثني لتطبيقات النطاق العريض باستخدام طرق عزل فعالة

اعداد: وطن فايز ظافر

اشراف: د. محمد كوعلي

ملخص:

إن الحاجة إلى إنتاج عناصر و أجهزة خفيفة الوزن و رخيصة الثمن هي القوة الدافعة باتجاه -macro electronics. لقد جذبت الإلكترونيات التي يمكن مدها و / أو مطابقتها للأسطح المنحنية اهتمامًا واسعًا مؤخرًا ، لذا تمت دراسة بعض microwave components في أطروحتنا.

في هذا العمل ، تم طرح تصميم لهوائي monopole مستطيل مطبوع لتطبيقات النطاق العريض (UWB). تم تصميم الهوائي المطبوع باستخدام برنامج HFSS لتحقيق أفضل معامل ارتداد. علاوة على ذلك ، تمت دراسة تأثير المط على استجابة الهوائي على طول المحور السيني والمحور الصادي. كما تم تصميم هوائيات compact UWB MIMO. من أجل تحسين impedance matching و العزل، يُقترح أن كل هوائي UWB MIMO يتكون من two comparable monopole elements يتم تصميه بعمل قطوع في المستوى الأرضي له. وقد تم تحليل معامل الارتداد mutual coupling معامل التكبير وأنماط الإشعاع.

TABLE OF CONTENTS

List of Figures

List of Tables

List of Acronyms

MIMO	Multi-Input Multi-Output
UWB	Ultra-Wide Band
LTE	Long Term Evolution
HFSS	High Frequency Structure Simulator
PDMS	Polydimethylsiloxane
AgNWs	Silver Nanowires
IMTS	The Improved Mobile Telephone Service
AMPS	Mobile Phone System
FCC	Federal Communication System
USDS	United States Digital System
TDMA	Time division multiple Access
GSM	Global System for Mobile
WLANs	Wireless Local Area Networks
DBS	Direct Broadcast Satellite
GPS	Global Positioning Satellite
HPBW	the Half Power Beamwidth
VSWR	Voltage Standing Wave Ratio
MMICs	Microwave Monolithic Circuits
RFID	Radio Frequency Identification

Chapter 1

Introduction

Chapter One

Introduction

The objective of this chapter is to present the purpose of the thesis;jh this chapter consists of motivation, statement of the problem that we want to solve, the literature review, and our contribution in this field.

1.1 Motivation

The need to produce light weight and cheap components and devices has been the driving force for macro-electronics. In recent years, the significant attention has focused on wearable system for monitoring human health and detecting human motions. By Using the wearable wireless communication, we can provide remote diagnosis and transmit the sensory data, and the antenna is a critical component for wireless communication.

Rigid antenna fails to work properly when it is under mechanical deformation, so development of stretchable and flexible antenna leads for new device configurations. Silver nanowires (AgNWs) are a promising material for flexible, transparent and stretchable components including solar cells, sensors, and flexible antennas.

1.2 Problem Statement

The aim of this thesis is to design a stretchable and reversely deformable Multi Input Multi Output Ultra-Wideband (MIMO UWB) antenna for Long Term Evolution (LTE), 5^{th} generation

and Wi-Fi applications. A literature study about stretchable microwave components and MIMO UWB antenna will introduce the main points of our design. High Frequency Structure Simulator (HFSS) will be used for the design and simulation. The antenna should operate on the UWB frequencies from 3.1 to 10.6 GHz, other wireless applications may need a wider band in addition to UWB band.

1.3 Literature Review

In order to understand the art of antenna design, UWB antennas and MIMO UWB antennas are investigated as literature review. Studies and papers about monopole patch antenna, MIMO UWB antenna and stretchable antennas deserved our attention and our research for this literature review. There are a lot of UWB antenna designs and the monopole rectangular patch was nearly the simplest one and suitable for many applications because of light weight, low cost, small size and other advantages. Mainly, we were influenced by two scientific papers; ‘’Stretchable and Reversibly Deformable Radio Frequency Antennas Based on Silver Nanowires’’ [1] and the other one is ‘’Design of High-Isolation Compact MIMO Antenna for UWB Application’’ [2].

1.3.1 Stretchable and Reversibly Deformable Radio Frequency Antennas Based on Silver Nanowires

In Stretchable and Reversibly Deformable Radio Frequency Antennas Based on Silver Nanowires paper, A class of microstrip patch antennas which are stretchable and reversibly deformable were presented, simulated and demonstrated. A highly conductive and stretchable material was used for the radiating element and the ground plane, Silver Nanowires (AgNWs), and an elastomeric material for the substrate, Polydimethylsiloxane (PDMS). These antennas are

a microstrip patch antenna and a 2-element patch array. The radiating properties agree with the simulation result which are characterized under stretching.

In our thesis, a monopole UWB patch antenna was designed and simulated using HFSS with PDMS/AgNWs materials. The tensile strain was applied along x-axis and y-axis to study its effects on the antenna parameters.

1.3.2 Design of High-Isolation Compact MIMO Antenna for UWB Application

In Design of High-Isolation Compact MIMO Antenna for UWB Application paper, a compact MIMO antenna for UWB communication applications was presented. The antenna consists of 2 identical monopole antennas and the isolation was improved with a comb-line structure on the ground plane. Different parameters were simulated and which showed that the presented UWB MIMO antenna is a good choice for UWB MIMO systems.

In our work, the monopole UWB patch antenna with same dimensions was used to create a 2 element MIMO antenna and the isolation was improved by introducing different stubs in the ground plane to minimize and enhance the mutual coupling between the 2 ports lower than -25 dB.

1.4 Thesis Contribution

In our work, a monopole UWB antenna from stretchable materials (PDMS/AgNWs) will be designed and simulated. It's effectiveness and efficiency will be checked under stretching to use in wearable systems like wearable health technologies, wearable textile technologies, and wearable consumer electronics. The other geometry is a compact MIMO UWB antenna which will be introduced using PDMS/AgNWs with different stubs to improve and minimize the mutual coupling between elements and achieving compact size.

Chapter 2

Antenna in Wireless Communication

Chapter Two

Antenna in Wireless Communication

In 1897, Marconi succeeded to provide a continuous contact across the English Channel between ships using radio waves. Since then, huge numbers of experiments were made in different labs by different researchers trying using the electromagnetic waves to transmit information and develop the field of wireless communications.

2.1 Evolution of Antennas and Wireless Communication Systems

Firstly, the public mobile telephone service was introduced in twenty-five major American cities, in the year 1946. This system covered a distance up to 50 Km using a single, high-powered transmitter with high tower, and half duplex channel with 120 KHz bandwidth, only 3KHz of this spectrum was required. During 1950s, the channel bandwidth was cut to be 60 KHz and finally, by the mid of 1960s, the channel was cut to be 30 KHz. By this time, The Improved Mobile Telephone Service (IMTS) which has automatic channel trunking and offered full duplex phone systems was introduced [3].

During the 1950s and 1960s, the technique of cellular radio telephony was developed. According to this concept, the coverage area was broken into small cells, and to increase spectrum usage, the concept of frequency reuse is applied. In 1983, channels for the Advanced Mobile Phone System (AMPS) were allocated by the Federal Communication Commission (FCC) in the range of 824-894 MHz The first digital system was installed in 1991 in United States (US) and it was called the US Digital System (USDS) and like AMPS, it used the same

frequency range with a digital modulation along with Time Division Multiple Access (TDMA) to improve the capacity by three times.

Historically, using RF energy for wireless communication began with the theoretical work of Maxwell, verified by the experiments of Hertz for electromagnetic wave propagation, and practical radio system development by Marconi in the early part of 20^{th} century. The wireless telegraphy was the first radio system. In 1988, the Global System for Mobile Communications GSM was insert in Europe and it was the first digital cellular system. North America IS-54 digital standard followed GSM.

Antenna engineering was being an important part of the emerging wireless technology, and the period between 1940s-1990s was a very successful period. During that period, some new elements of radiation were introduced and developed like reflectors, aperture antennas, micro strip antennas, and frequency independent antennas. Integration of new materials into the antenna technology offers many opportunities. Modeling complex electromagnetics wave interactions is now possible using supercomputing and parallel computing capabilities, in both time and frequency domains [4].

Today, wireless systems include cellular telephone systems, broadcast radio and television, Wireless Local Area Networks (WLANs), global weather, Direct Broadcast Satellite (DBS) television service, Global Positioning Satellite (GPS) service and others. Wireless devices are everywhere at the present, which will provide worldwide connectivity for voice, video and data communications. The growing wireless area performs an equally important role in private and consecrated communication systems [5].

In recent years, new types of antennas were invented such as smart antennas. Smart antennas (also known as multiple antennas or adaptive array antennas) now regarded as one of enabling technologies for next-generation wireless communication systems [6].

2.2 How an Antenna Radiates

Antenna is a metallic structure intended for radiating and receiving electromagnetic waves [4]. We need to consider how radiation occurs so as to know how an antenna transmits. When we have mainly a time-varying current or acceleration or deceleration of charge, a conducting wire radiates. If there is no motion of charges or no flow of current occurs or charges have a uniform velocity on a straight wire, no radiation happens. If the charge is wavering with time, then radiation takes place even along a straight wire as clarified by Balanis [4].

If we have a look on Figure 2.1, we can understand how the radiation occurs. The electric field which is sinusoidal in nature will form, when a sinusoidal voltage is applied to the transmission line. The electric lines will cause the flow of current because of a movement of the free electrons on the conductor and the magnetic field will create.

Now we have a time varying electric and magnetic fields, which will create electromagnetic waves which will travel between the conductors. Free space waves are formed when the electromagnetic waves reach the open space. Continuously, the electromagnetic waves are formed and travelled from the transmission line to reach the free space through the antenna. Through the antenna and the transmission line, because of the charges, the electromagnetic waves are incessant and as soon as they reach the free space, closed loops will be formed and radiated [4].

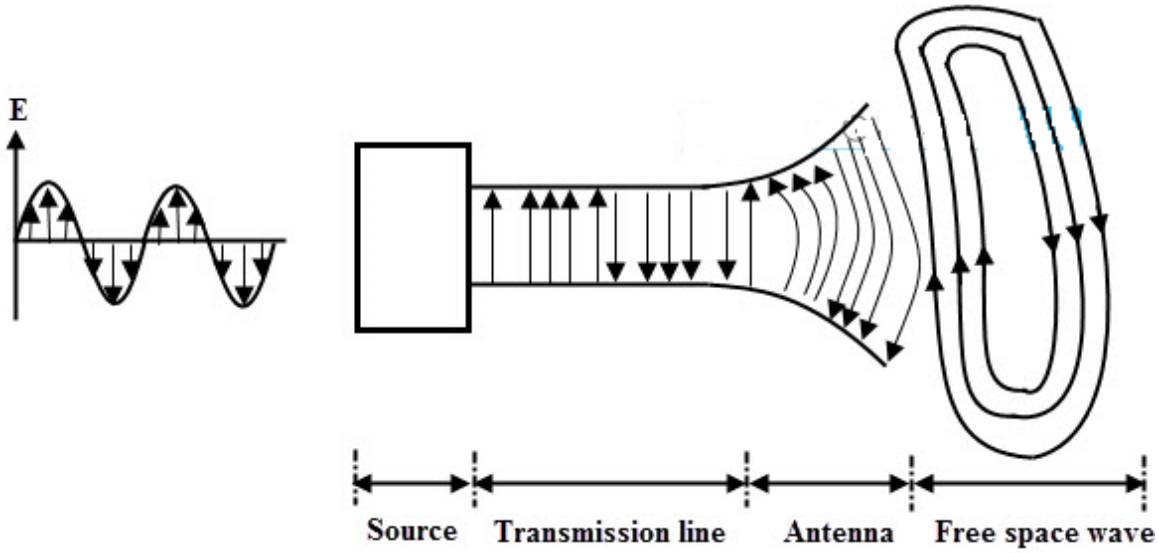

Figure 2.1 Radiation from an antenna [4].

2.3 Near and Far Field Regions

There are three regions in the space surrounding an antenna:

1. Reactive near field region
2. Radiating near field region
3. Far field region

As shown in Figure 2.2, the field patterns, change with distance and are associated with two types of energy: reactive energy and radiating energy.

The reactive field dominates in the reactive near-field region. The reactive energy oscillates towards and away from the antenna, thus appearing as reactance. There is no energy dissipation and the energy is only stored in this region. The boundary for this region is at a distance of

$$R_1 = 0.62\sqrt{D^3/\lambda} \tag{2.1}$$

where:

$\boldsymbol{R_1}$ is the distance from the antenna surface,

$\boldsymbol{D}$ is the largest dimension of the antenna and

$\boldsymbol{\lambda}$ is the wavelength.

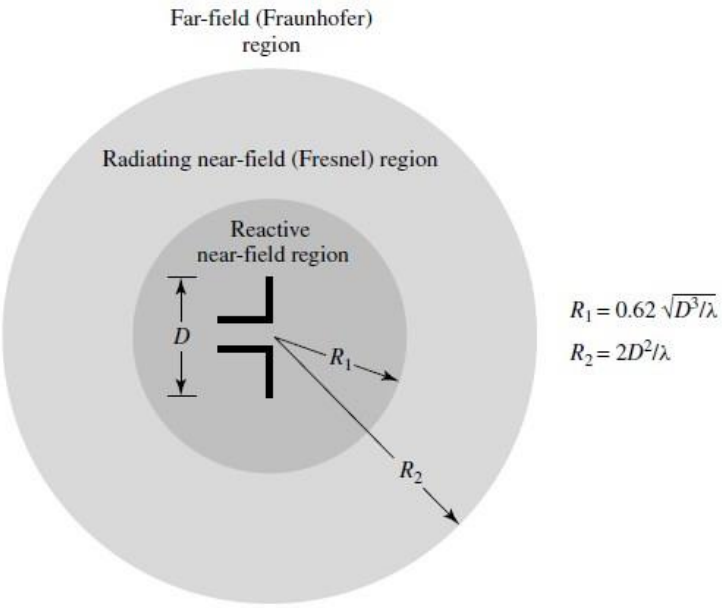

Figure 2.2 Field regions around an antenna [4].

The Fresnel region, which is the radiating rear-field region, stands between the far field and reactive near-field regions. In this region the reactive fields are small and the radiation fields are the dominant fields. The boundary for this region can be given by:

$$R_2 = 2D^2/\lambda \tag{2.2}$$

Where:

$\boldsymbol{R_2}$ is the distance from the antenna.

Finally, the far-field region, which is called the Fraunhofer region, locates at a distance greater than $2D^2/\lambda$. In this region, the radiation fields exist and its distribution isn't dependent on the distance from the antenna. Also, the power density inversely proportional by the square of the radial distance.

2.4 Antenna Performance Parameters

Different parameters can be used to demonstrate the performance of an antenna like Radiation Pattern, Radiation Power Density, Directivity, Antenna Efficiency, Antenna Gain and others.

2.4.1 Radiation Pattern

The radiation pattern means a graphical representation or the form of the power radiated from the antenna in the space. In some cases, it is located or specified in the far-field region. Radiation includes power density, radiation intensity, directivity and polarization. Patch antenna radiated power in free space as shown in Figure 2.3 below.

If we consider the isotropic antenna, which radiates evenly in all directions, the total radiated power is ***P***. We can calculate the power density w_{rad} at any distance and any direction using:

$$w_{rad} = \frac{P}{area} = \frac{P}{4\pi r^2} \tag{2.3}$$

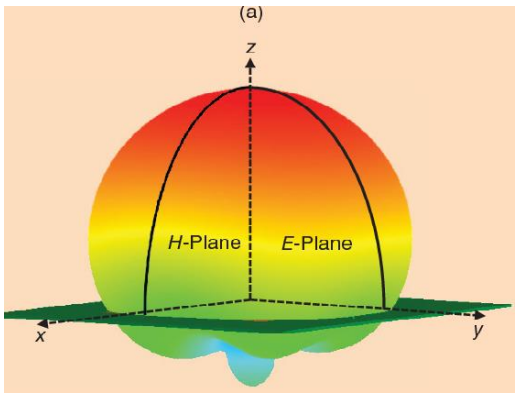

Figure 2.3 radiation pattern of a patch antenna [7].

Then the isotropic antenna has a radiation intensity *U* which can be written as:

$$U_i = r^2 w_{rad} = P/4\pi \tag{2.4}$$

The plot of the radiation power plot of a directional antenna is shown in Figure 2.4. It consists of a main lobe and some minor lobes. The major lobe occurs at the direction of maximum radiation and the other minor lobes are present the radiation in undesired directions. And the Half Power Beamwidth (HPBW) is the angle subtended by the half power points of the main lobe.

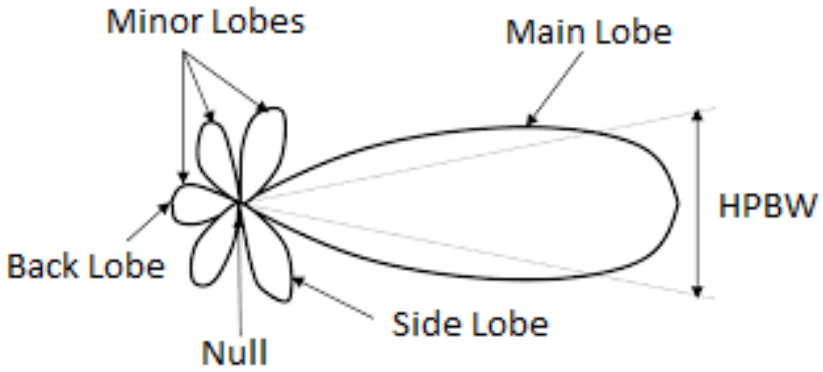

Figure 2.4 Radiation pattern of a generic directional antenna [4].

2.4.2 Radiation Power Density

We can find the power density through the electric and magnetic field, and here the current is important to create the potential, and from it we find the electric and magnetic field, now the equation below describes the relationship between the Poynting vector which is the quantity used to describe the power associated with an electromagnetic wave.

$$W = E \times H \tag{2.4}$$

Where:

W is the instantaneous Poynting vector (W/m^2)

E *is* the instantaneous electric-field intensity (V/m)

H is the instantaneous magnetic-field intensity (A/m)

The total power crossing a closed surface given by:

$$p = \oiint_s W.ds = \oiint_s W.\hat{n}\, da \tag{2.5}$$

Where:

$\boldsymbol{p}$ is the instantaneous total power (W).

$\hat{\boldsymbol{n}}$ is the unit vector normal to the surface.

a *is* the infinitesimal area of the closed surface (m^2).

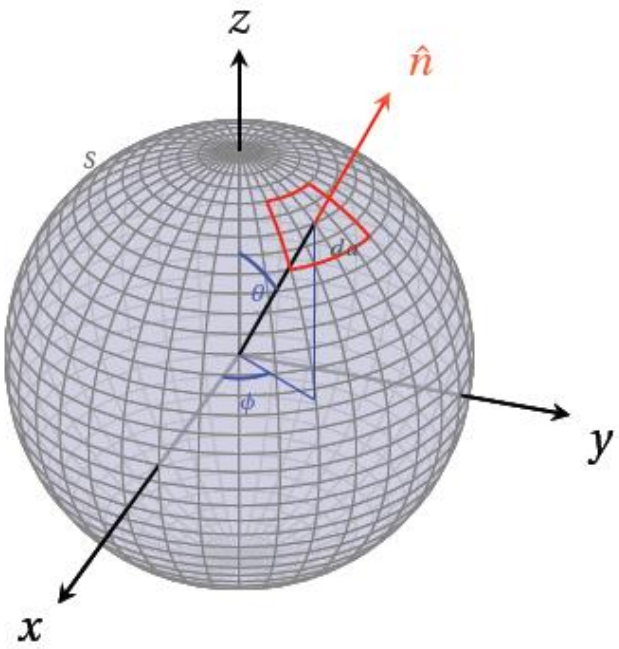

Figure 2.5 Geometrical arrangement for defining the normal of the surface

The power density of an antenna is mostly real and will be referred to as *radiation density* and can be written as:

$$p_{rad} = p_{av} = \oiint_s w_{rad}.ds = \oiint_s w_{av}.\hat{n}\, da$$

$$= \frac{1}{2}\oiint_s R_e[E \times H^*].ds \tag{2.6}$$

2.4.3 Radiation Intensity

The radiation intensity means that "the power radiated from an antenna per unit solid angle" [4]. And the radiation intensity is applied in a far-field region, and it can be obtained by the equation below.

$$U = r^2 W_{rad} \quad (2.7)$$

Where:

U is the radiation intensity (W/unit solid angle)

$\boldsymbol{W_{rad}}$ is the radiation density (W/m^2)

2.4.4 Antenna Efficiency

Antenna efficiency describes the effective amount of the antenna. And the antenna may be loss power due to reflection, this means mismatch impedance which is happen between the antenna and transmission line, this description generalized in Figure 2.6 below.

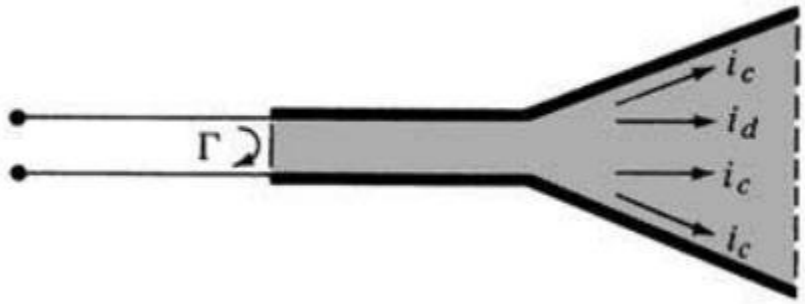

Figure 2.6 Reflection conduction and dielectric losses [4].

In general, the total efficiency is written as:

$$e_0 = e_r e_c e_d \quad (2.8)$$

Where:

$\boldsymbol{e_0}$ is the total efficiency (dimensionless)

$\boldsymbol{e_r}$ is the reflection (mismatch) efficiency = $(1 - |\Gamma|^2)$ (dimensionless)

$\boldsymbol{e_c}$ is the conduction efficiency (dimensionless)

$\boldsymbol{e_d}$ is the dielectric efficiency (dimensionless)

Γ is the voltage reflection coefficient at the input terminals of the antenna

$\Gamma = (Z_{in} - Z_0))/(Z_{in} + Z_0)$ where Z_{in} = antenna input impedance

Z_0 is the characteristic impedance of the transmission line.

2.4.5 Gain

Another parameter portrays the performance of an antenna is the gain. That is closely depended on the directivity, the reliability between the directivity and gain represented by the efficiency parameter and the gain occurs inside the antenna. In contrast the directivity. In equation for this can be expressed as:

$$Gain = 4\pi \boldsymbol{U}(\boldsymbol{\theta}, \boldsymbol{\varphi})\, \boldsymbol{Pin} \tag{2.9}$$

2.4.6 Directivity

The antenna directivity is presented as the ratio of the radiation intensity in a given direction to the average radiation intensity which is equal to the total power transmitted by the antenna divided on 4π.

In different definition, the directivity of a non-isotropic source is match to the proportion of its radiation intensity in a provided direction, over that of an isotropic source. So, the directivity can be given by:

$$D = \frac{U}{U_0}$$

$$= \frac{4\pi U}{Prad} \tag{2.10}$$

Where:

$\boldsymbol{D}$ is the directivity of the antenna

$\boldsymbol{U}$ is the radiation intensity of the antenna

$\boldsymbol{U_0}$ is the radiation intensity of an isotropic source

$\boldsymbol{P_{rad}}$ is the total radiated power

2.4.7 Voltage Standing Wave Ratio (VSWR)

In order to operate efficiently, the antenna should have a maximum power transfer between the antenna and the transmitter. This can happen only when the impedance of the antenna (Z_{in}) is matched to the impedance of the transmitter (Z_s). According to this theorem, the impedance of the antenna is a complex conjugate to that of the transmitter, and then the maximum power can be transferred and vice-versa. Thus, the condition is:

$$Z_{in} = Z_s^* \tag{2.11}$$

If matching condition isn't achieved, then part of the power will be reflected and this will create a standing wave, which is described by the Voltage Standing Wave Ratio (VSWR). The VSWR is given by:

$$VSWR = \frac{1+|\Gamma|}{1-|\Gamma|} \tag{2.12}$$

$$\Gamma = \frac{V_r}{V_i} = \frac{Z_{in} - Z_s}{Z_{in} + Z_s} \tag{2.13}$$

Where:

$\boldsymbol{\Gamma}$ is called the reflection coefficient,

$\boldsymbol{V_r}$ is the amplitude of the reflected wave and

$\boldsymbol{V_i}$ is the amplitude of the incident wave

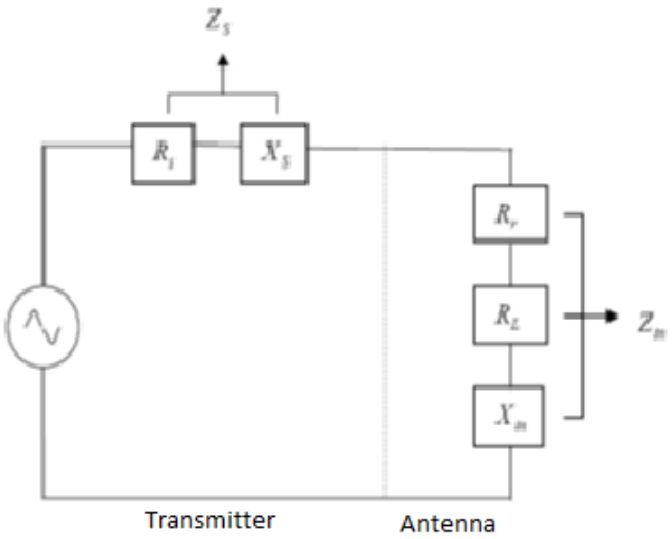

Figure 2.7 Equivalent circuit of transmitting antenna [4].

The VSWR is mainly a measure of the mismatch between Z_s and Z_{in}. As the VSWR increases, the mismatch increases. When we have a perfect match, the minimum VSWR is unity. Most radio equipment is built for either 50 Ω or 75 Ω, so a practical antenna design to have these impedances.

2.4.8 Reflection Coefficient

In telecommunications, there are different coefficients to judge the system one of them is the reflection coefficient, which is the ratio of the amplitude of the reflected wave to the amplitude of the incident wave. In particular, at a discontinuity in a transmission line, it is the complex ratio of the reflected voltage (V-) to that of the incident voltage (V+).

This is typically represented with Γ as:

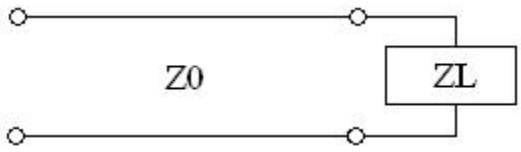

Figure 2.8 Transmission line circuit

$$\Gamma = \frac{V-}{V+} \tag{2.14}$$

The reflection coefficient can be given by the equations below:

$$\Gamma = \frac{z_l - z_0}{z_l + z_0} \tag{2.15}$$

Where:

z_l is the impedance toward the load and

z_0 is the impedance toward the source

From the previous equation, the magnitude of the reflection coefficient depends only on the impedance of the transmission line and the load impedance. The absolute magnitude of the reflection coefficient can be calculated from the standing wave ratio (SWR) using:

$$|\Gamma| = \frac{SWR-1}{SWR+1} \tag{2.16}$$

2.4.9 Return Loss

S-parameters describe the input-output relationship between ports or terminals in an electrical system. For instance, if we have 2 ports (Port1 and Port2), then S_{12} represents the power transferred from Port 2 to Port 1, S_{21} represents the power transferred from Port 1 to Port 2. In practice, the most commonly quoted parameter in regards to antennas is the return loss (S_{11}). Return loss RL represents how much power is reflected from the antenna. The RL is given as [8]:

$$RL = 20log\,|\Gamma| \tag{2.17}$$

To achieve matching, no power would be back, from the antenna to the transmitter, Γ = 0 and $RL = \infty$, whereas a Γ = 1 has a RL = 0 dB, which means the reflection of all the incident power. In reality, a VSWR of 2 is acceptable, which means that the RL is 9.54 dB.

2.5 Types of Antennas

The antennas of wireless applications have various shapes and sizes. The attributes of it are significantly determined by its shape, size, beamwidth and the kind of material that it is made of. Some of the common antennas are shortly expounded in the next subsections.

2.5.1 Wire Antennas

This is the oldest, simplest, cheapest and the most multilateral type of antenna for many applications [9]. This kind of antenna has different shapes, wire antenna may be:

1. Linear wire antenna: this antenna has a straight wire form and also called as a dipole antenna and a monopole antenna which is half of a dipole antenna on top of a conducting ground plane.
2. Loop antenna: when the wire is shaped as a loop, it is called loop antenna. This loop can take any shape like a circle, square, rectangular and others shape.
3. Helical antenna : a wire has a helical shape, the antenna called helical or simply helix.

2.5.2 Aperture Antennas

A horn antenna is an example of aperture antennas. These antennas are formed from the waveguide which is a hollow metallic structure through which waves travel. It is either rectangular or circular waveguide. Typically, it is used in the microwave zone which is mainly supplied using waveguides method.

Horn antennas have a high gain, relatively wide bandwidth, low VSWR, light weight, and easy to build. However, rectangular horns are widely used. Figure 2.9 shows three basic utilization for a rectangular geometry.

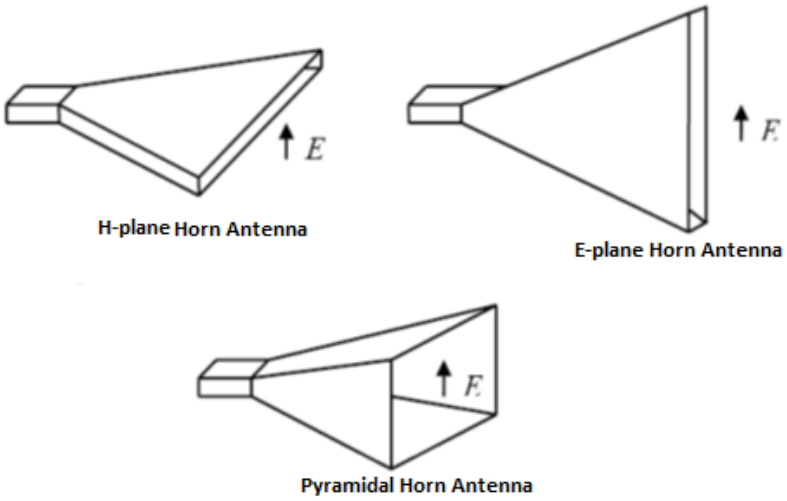

Figure 2.9 Types of horn antenna [4].

This kind of antennas is widely used as a feed element for communication dishes, satellite tracking, and large radio astronomy.

2.5.3 Microstrip patch Antennas

This antenna having three layers, the top layer is a patch which is from a conducting material etched on one side of a dielectric substrate and the other side of the substrate etched with a metal ground plane. The radiating patch may take different shapes like rectangular, square, circular etc. This kind of antennas are suitable for space craft. We consider this kind of antennas in our thesis.

2.5.4 Reflector Antennas

These antennas carry with it a radiating element beside a reflecting surface. Simply, the dipole acts as a radiating element and a flat conductor as a reflector which will improve the directivity. The periodic reflector is one of the popular forms of reflector antenna which use a periodic reflector instead of the flat reflector.

2.5.5 Lens Antennas

The lenses are used to collecte the incident divergent light energy preventing it from spreading in different directions. Similarly, it can be used to transfer various forms of waves energy into plane waves. Particularly, it is suitable at higher frequencies like parabolic dish and used as wide band antenna.

Chapter 3

Microstrip Patch Antenna

Chapter Three

Microstrip Patch Antenna

In superior applications like craft, satellite, and missile applications, where size, weight, performance, cost, and simple installation and fabrication, low-profile antennas could also be needed. Nowadays there are several alternative governments and industrial applications, like wireless communications and mobile radio that have similar specifications. To fulfill these needs, microstrip antennas will be used [4].

3.1 History

In 1950s, the first microstrip antenna was introduced, but to be realized, it had to wait nearly 20 years after developing the printed circuit board technology. Nowadays, microstrip antennas are the foremost common kind with big selection of applications thanks to their advantages starting from its light weight and ending with integration with Microwave Monolithic Circuits (MMICs) and other advantages. They have been greatly involved for the civilian and military applications such as Radio Frequency Identification (RFID), multiple-input multiple-output systems, and so on [10].

3.2 Basic Characteristics

Microstrip antenna, as shown in Figure 3.1, has three layers, the first one is a very skinny ($t \_ \lambda 0$, where $\lambda 0$ is the wavelength of the free-space) metallic strip (patch) placed on a dielectric substrate of a little fraction of a wavelength ($h \_ \lambda 0$, usually $0.003\ \lambda 0 \leq h \leq 0.05\ \lambda 0$) on the top of a ground plane.

It has a maximum radiation pattern normal to its plane (broadside radiator), but we have to choose a proper field configuration (mode) of excitation beneath the patch. Using judicious mode selection, the end-fire radiation can also be accomplished. The length of a rectangular patch L is usually $\lambda 0/3 < L < \lambda 0/2$. A dielectric sheet (the substrate) separates between the patch and the ground plane.

There are numerous materials for the substrate that can be used, and their dielectric constants are usually between $2.2 \leq \epsilon_r \leq 12$. For good antenna performance, the dielectric constant of a thick substrate is in the lower end of this range to provide better efficiency, larger bandwidth, but we will have a larger element size [4].

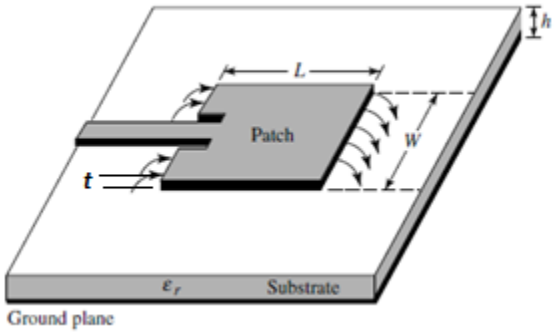

Figure 3.1 patch antenna [4].

The microstrip antennas are also called as *patch* antennas. The feed lines and the radiating elements are the upper layer, which usually printed on the dielectric substrate. The radiating element may be rectangular, square, circular, thin strip (dipole), triangular, elliptical, or any other configuration.

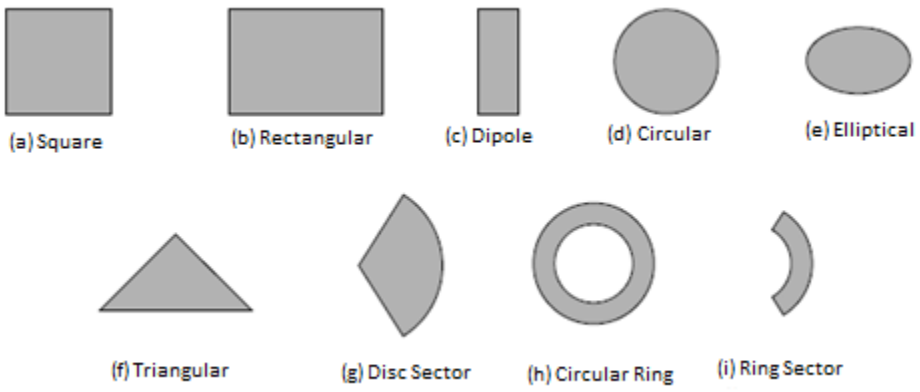

Figure 3.2 Some shapes of the patch elements [4].

3.3 Feeding Methods

In Microstrip patch antenna, there are many different techniques of feeding methods, in rectangular microstrip patch antenna the most common type is the Microstrip feed line, coaxial probe and we can also use the electromagnetic coupling or aperture coupling waveguide feeding.

3.3.1 Microstrip Feed Line

Microstrip feed line is depending on the conducting strip. Using this technique, a connecting strip is connected to the patch directly, and therefore it can be considered as an extension of the patch. Simply it can be modeled and easily matching by controlling the inset position. However, the disadvantage of this method is the limit of bandwidth when the substrate thickness increases, surface wave and spurious feed radiation increase. A Microstrip feed line shown in Figure 3.3 which was used to feed our antennas.

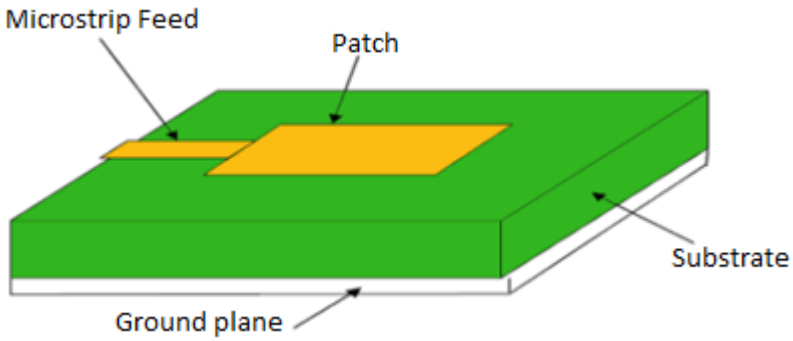

Figure 3.3 Microstrip line feed [11]

3.3.2 Coaxial Feeding

The Coaxial feeding, also known as probe feed, is a method in which that the inward conduit of the coaxial stretches out through the dielectric and is connected to the radiating patch, and the external conductor will be associated with the ground plane. A Coaxial feed model shown in Figure 3.4.

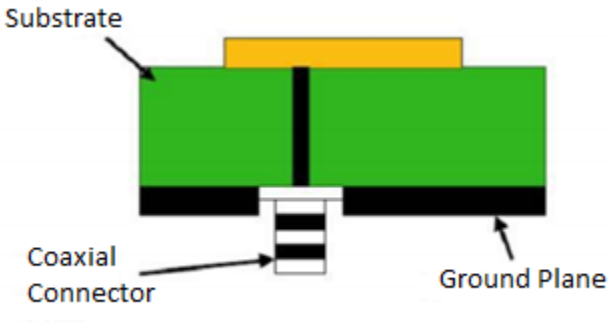

Figure 3.4 Coaxial Fed Rectangular Microstrip Patch Antenna [11]

3.3.3 Aperture Coupling

The aperture coupling is the other method of feeding. In this technique, as shown in Figure 3.5, the transmission of energy to the antenna is done by the feed line which is covered from the antenna by a conducting plane with a hole (aperture).

In this method, the substrate consists of two layers. The upper layer is made from a low permittivity material producing a loosely bound fringing fields, and better radiation and the

lower one is made with a high permittivity material for tightly coupled fields to avoid producing spurious radiation. Increasing difficulty in fabrication is the disadvantage of this method.

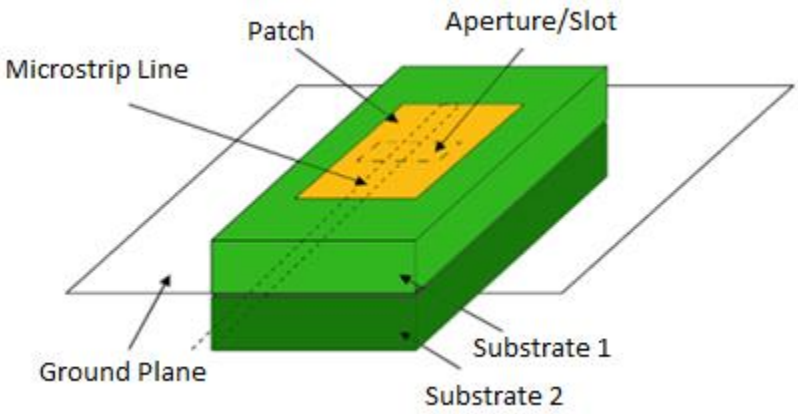

Figure 3.5 Aperture coupled feed [11]

3.3.4 Proximity Coupling

In the mid-to-late 1980s, new techniques for feeding the microstrip antennas, which are noncontact techniques, were inserted. Since then, several of the performance obstruction related with direct contact techniques were defeated by aperture coupling and proximity coupling. Proximity coupled patches have received little attention. This may be because the original form required an external impedance matching circuit to achieve a reasonable impedance [12].

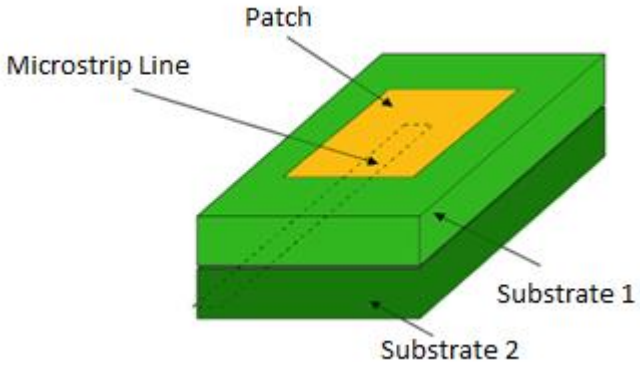

Figure 3.6 Proximity coupling feed [11]

3.4 Radiation Mechanism

As shown in Figure 3.7, when a power is provided to the microstrip patch, the upper and the lower surfaces of the batch will have a charge distribution and at the base of the ground plane. This distribution of the charge is constrained by the repulsive mechanism and the attractive mechanism. The similar charges fall under the influence of the repulsive mechanism on the bottom surface of the patch, currents flow at the two surfaces of the patch due to pushing some charges from the bottom to the top of the patch.

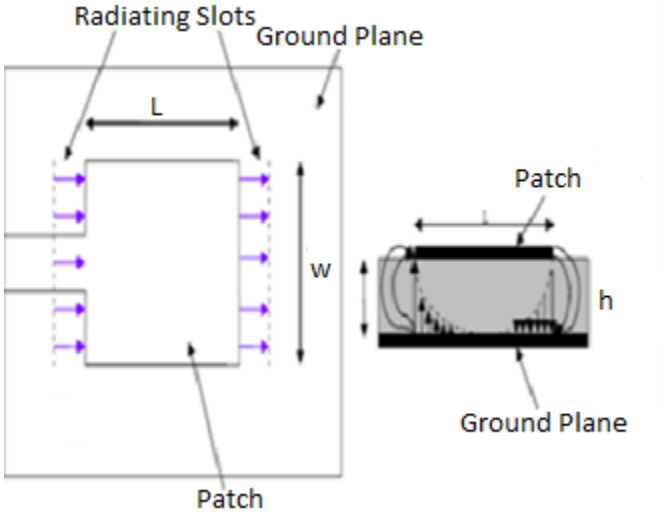

Figure 3.7 Radiation mechanism of microstrip patch antenna (Top and side view) [13]

The opposite charges on the ground plane and on the bottom side of the patch are controlled by the attractive mechanism, by this mechanism, the charge concentration keeps intact at the bottom of the patch. Refer to Figure 3.7, the patch is represented by two slots, which separeted by L of a transmission line and open circuits at the ends. The voltage is maximum and the current is minimum along the width of the patch. The fields at the edges have normal and tangential components with respect to the groung plane. The normal components of the electric field along the width are out of phase and hence it will be zero. The radiation field is normal to the surface of the antenna because of the in phase tangential components [13].

The edges of the width can be assumed as two radiating slots, spaced by $\lambda/2$, excited in phase and radiating in the half space above the ground plane. Because of the fringing fields, electrically the microstrip patch antenna looks greater than its physical dimensions. The cavity model According to the cavity model, the hieght of the substrate to the width of the patch ratio is very small, so the domination will be to the attractive mechanism. As a result, the current and charge concentration will be below the patch surface and the top surface of the patch will have much less current flow. The current on the top surface of the patch is directly proportional to this ratio. At the edges, there is no creation of the tangential magnetic field components. Hence, the sidewalls are perfectly magnetic conducting surfaces.

Actuality, this ratio would be exist and the tangential magnetic fields would be very small. Since the walls of the cavity, as well as the material within it are lossless, the cavity would not radiate and its input impedance would be purely reactive.

3.5 Rectangular Microstrip Patch

The rectangular patch is one of the foremost widely used antenna. The transmission-line and cavity models are using to analyze it easily, which are most accurate for thin substrates. We use with the transmission-line model because it is easier to illustrate [4].

3.5.1 Transmission-Line Model

The transmission-line model is the easiest one but it yields the least accurate results and it lacks the versatility. Basically, the transmission-line model represents the microstrip antenna by two slots, separated by a low-impedance *Zc* and a transmission line of length *L*.

A. Fringing Effects

Because the length and width of the patch have finite dimensions, the fields at the edges of the patch undergo fringing. This is illustrated along the length in Figures 3.8 for the two radiating slots of the microstrip antenna. The same happens along the width. The amount of fringing is dependent on the dimensions of the patch and the height of the substrate. This is a nonhomogeneous line of two dielectrics; the substrate and air. As we can see, most of the electric field lines lie in the substrate and parts of some lines exist in air.

Duo to the Fringing, the microstrip line looks wider electrically compared to its physical dimensions. Because some of waves travel in the substrate and some in air, an *effective dielectric constant* ϵ_{reff} is introduced to account for fringing and the wave propagation in the line.

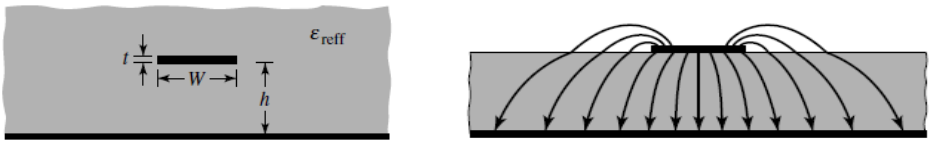

Figure 3.8 Microstrip line and its electric field lines, and effective dielectric constant geometry [4].

The effective dielectric constant at low frequencies is actually constant. At intermediate frequencies its values begin to monotonically increase and finally approach the dielectric constant value of the substrate. The initial values of the effective dielectric constant are named as the *static values* which given by:

$$\frac{w}{h}>1$$

$$\epsilon_{reff} = \frac{\epsilon_r+1}{2} + \frac{\epsilon r-1}{2}[1 + 12\frac{h}{w}]^{-1/2} \qquad (3.1)$$

B. Effective Length, Resonant Frequency, and Effective Width

The electric length of the patch looks greater than its actual dimensions because of fringing effects. For the principal *E*-plane (*xy*-plane), it is demonstrated in Figure 3.9. The dimensions of the patch along its length have been extended on each end by a distance *3L*, this length extension is a function of the effective dielectric constant I_{reff} and the width-to-height ratio (*W/h*). Equation 3.10 shows a very popular and practical approximate relation for this normalized extension of the length [4].

$$\frac{\Delta L}{h} = 0.412 \ \frac{(\epsilon_{reff}+0.3)(\frac{W}{h}+0.264)}{(\epsilon_{reff}-0.258)(\frac{W}{h}+0.8)} \tag{3.2}$$

The length of the patch has been extended by *3L* on each side, so the effective length of it is (*L* = *λ*/2 for dominant TM_{010} mode with no fringing).

$$L_{eff} = L + 2\Delta L \tag{3.11}$$

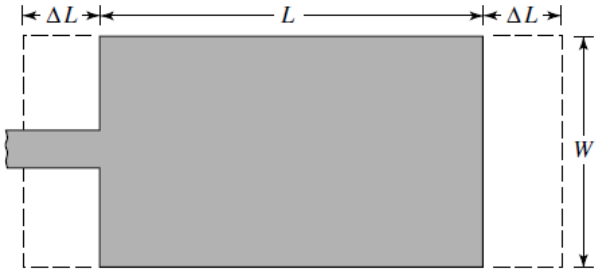

Figure 3.9 Physical and effective lengths of a rectangular microstrip patch [4].

For the dominant TM_{010} mode, the microstrip antenna has a resonant frequency which is a function of its length. Usually it is given by:

$$(f_r)_{010} = \frac{1}{2L\sqrt{\epsilon_r}\sqrt{\mu_0}\sqrt{\mu_0}\sqrt{\epsilon_0}} = \frac{v_0}{2L\sqrt{\epsilon_r}} \tag{3.3}$$

Where:

$\boldsymbol{v_0}$ is the speed of the light in free space.

ϵ_r is dielectric constant of the substrate.

Also, we need to determine the width of the patch using:

$$w = \frac{1}{2f_r\sqrt{\mu_0\epsilon_0}}\sqrt{\frac{2}{\epsilon_r+1}} = \frac{v_0}{2f_r}\sqrt{\frac{2}{\varepsilon_r+1}} \quad (3.4)$$

C. Design

To design a rectangular patch antenna, you need to specify dielectric constant of the substrate ϵ_r, the resonance frequency that you need fr, and the height of the substrate h. Finally, you can determine the width and the length of your design.

3.6 Applications of the Microstrip Antenna

Because its performance and design, the microstrip antenna is famous and widely used in different fields. Microstrip patch antennas have different applications in different fields such as satellites, military systems, and in medical field. The usage of it is spreading in all fields and they are blossoming in the commercial aspects thanks to their low cost and easy fabrication [14]. Some of these applications are mentioned below.

3.6.1 Satellite and mobile communication application

These applications require small, low cost, and low profile antennas. All these specifications are satisfied in microstrip patch antenna and that make this kind of antennas convenaient for mobile communication systems. If we use a square or circular patch, the radiation patterns will be circularly polarized which make it suitable for satellite communication.

3.6.2 Global positioning system applications

The U.S. Global Positioning System GPS is one of the Global Navigation Satellite Systems GNSS which is a constellation of satellites, transmitting signals anywhere on the surface of the earth [15]. Microstrip patch antennas are very compact, circularly polarized, have high permittivity substrate material and these features are important to develop efficient navigation devices.

3.6.3 Radio frequency identification (RFID)

In RFID, the electromagnetic fields are used to identify and track tags which contain electronically stored information and attached to fifferent objects. It is used in different applications from mobile communication to health care.

3.6.4 Bluetooth applications

Bluetooth applications operate on 2400 to 2484 MHz ISM Band, which is used for industrial, scientific and medical applications [16]. Microstrip patch antenna is preferred due to the smaller size and high efficiency.

3.6.5 Radar application

To detect moving people, vehicles and other things we use radar. Since 1970s, the microstrip patch antennas have developed from a patch structure to complex multilayer and array configurations. It meets all needs for radar applications like phased arrays, wide band transceiver technologies, small size and compacte structure [17]. So the microstrip patch antenna is an ideal choice for radar applications.

Chapter 4

Design and Simulation of Microstrip Patch Antenna for UWB Applications

Chapter Four

Design and Simulation of Microstrip Patch Antenna for UWB Applications

In recent years, the significant attention has focus on wearable system for monitoring human health and detecting human motions [18,19]. Using the wearable wireless communication, we can provide remote diagnosis and transmit the sensory data, and the antenna is a critical component for wireless communication [1].

Rigid antenna fails to work properly when it is under mechanical deformation, so development of stretchable and flexible antenna leads for new device configurations.

Silver nanowires (AgNWs) is a promising material for flexible, transparent and stretchable components including solar cells, sensors, and flexible antennas [20].

In this chapter a monopole UWB antenna from stretchable material (AgNWs for the patch and ground plates and PDMS for the substrate) will be designed. A review of the design process and applying the modeling and simulation using HFSS will be presented. The main antenna parameters will be measured and analyzed such that S parameter, Voltage Standing Wave Ratio VSWR, and finally the effects of changing the dimensions of the antenna under stretching will be analyzed.

4.1 Design of the proposed Antenna Using HFSS

In 2000, the Federal Communication Commission (FCC) issued a license for ultra wideband communication system for bandwidth of (3.1-10.6) GHz [21]. Since that time many microwave components have been implemented within the specified bandwidth, these components are:

Microwave filters, couplers and antennas. Many approaches have been introduced for ultra-wide band antenna; such examples include monopole microstrip antenna. The radiation pattern of this antenna has maxima in direction normal to surface of antenna at low frequencies, while it has maxima in other directions at high frequencies.

The proposed prototype of the compact monopole UWB antenna is shown in Figure 5.1. One antenna element is printed on a 16 mm X 18 mm stretchable PDMS substrate, with a thickness of 1mm and relative permittivity of nearly 2.8 and loss tangent ranging from 0.01 to 0.05. According to that, we modelled the substrate material with loss tangent of 0.02. The conductivity of the AgNWs/PDMS stretchable conductor is nearly 8130 Scm^{-1} before stretching [2]. AgNWs is used for the patch and the ground plates.

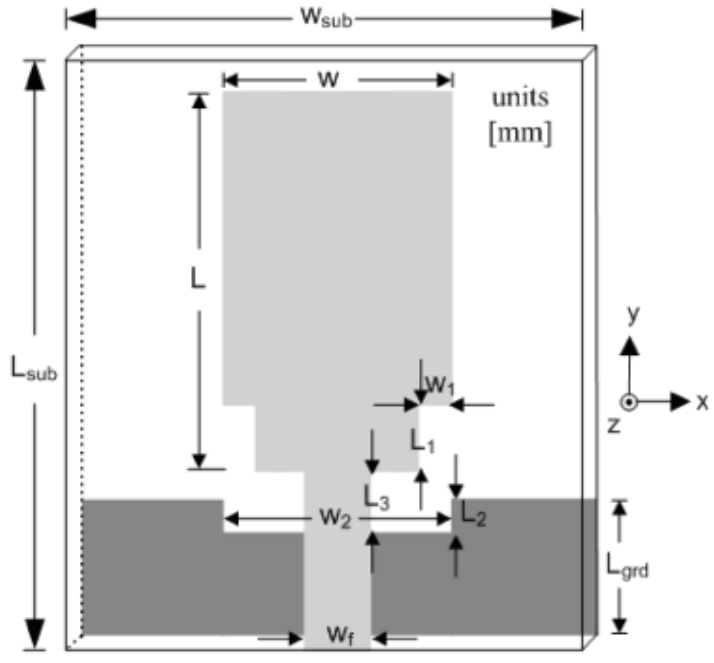

Figure 4.1 Monopole UWB antenna.

The UWB antenna consist of monopole antenna. The radiating element has a rectangular shape, and there is a symmetrical staircase structure on the two bottom corners of the radiating element.

To obtain the desired frequency, the rectangular patch was designed to be 7 mm X 11 mm, backed with an 18 mm X 5.9 mm ground plane. For matching the input impedance of a 2 mm X 6 mm 50 Ω microstrip feed line, a staircase structure was employed. Antenna dimensions were optimized in ANSYS HFSS v.13 to get the best return loss and increase the coupling between the patch and the feed line. The optimized dimensions for the UWB antenna are listed in Table 1.

Table 1. Dimensions of the proposed UWB antenna (mm).

w_{sub}	l_{sub}	w	L	w_1	l_1	w_2	l_2	w_f	l_3	l_{gnd}	h
16	18	7	11	0.5	1	9	1	2	1.1	5.9	2

4.2 Results and Discussion

4.2.1 Antenna Elements

The designed UWB antenna consists of a rectangular patch element. The monopole antenna was designed using a stretchable material, PDMS for the substrate and AgNWs for the top and ground plates. The optimal dimensions for the structure of the UWB antenna were shown in the previous section.

The UWB rectangular monopole patch antenna has approximately a lower resonance frequency at [23]

$$f_{rl} = \frac{144}{l_{gnd} + L + g + \frac{w_{sub}}{\sqrt{1+\varepsilon r}} + \frac{w}{\sqrt{1+\varepsilon r}}} \quad GHz \tag{4.1}$$

Where $l_{gnd}, L, and\ g$ are the length of the ground, the length of the radiating element and the gap between them respectively. The calculated f_{rl} is about 7 GHz. The simulated lower resonance frequency is about 5 GHz. Figure 4.2 shows the simulated $|S_{11}|$ which is less than -10 dB for the UWB operation.

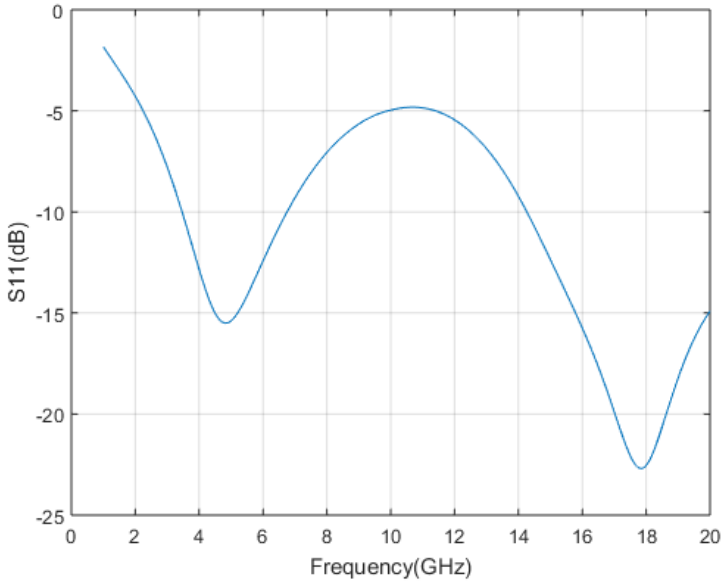

Figure 4.2 Simulated $|S_{11}|$.

For input impedance matching improvement and enhancement, the bandwidth of the antenna, a staircase structure is done and a rectangular slot is cut on the ground plane underneath each feeding line. By changing l_1 and w_1, the lower cut off frequency could be varied to reach 6 GHz and $|S_{11}|$ will be less than -10 dB from 3.37 GHz to 15.2 GHz which means that the staircase and the slot in the ground plate have a great effect on the input impedance matching as shown in Figure 4.3.

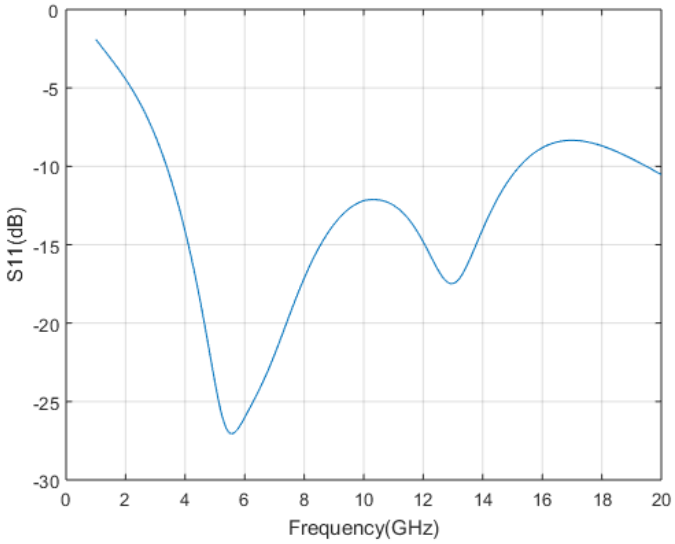

Figure 4.3 Simulated $|S_{11}|$ after doing staircase and ground slot.

After these improvements, the stretching is applied on the antenna along x-axis and y-axis, along its width and length respectively, the applied stretching was between (0-15) %. The value of S_{11} gives an indication about how the waves are reflected under stretching and how this affected antenna bandwidth. Figure 4.4 represents the value of S_{11} under stretching along x-axis and Figure 4.5 for S_{11} with stretching along y-axis. In UWB application it is acceptable when its value less than -10 dB continuously.

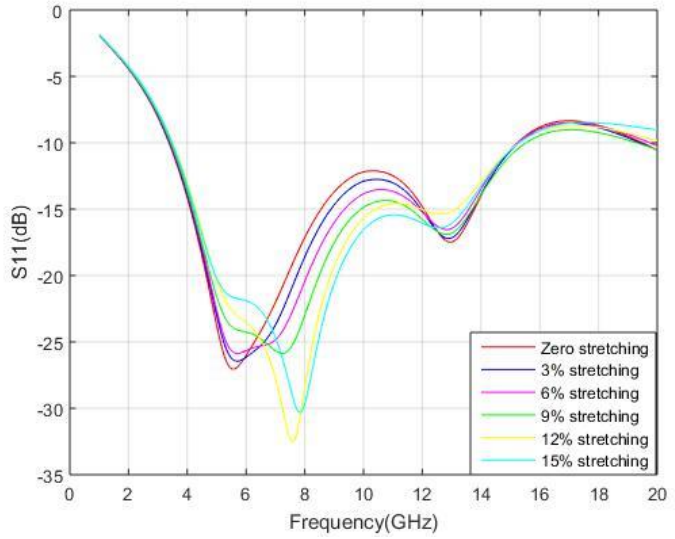

Figure 4.4 Simulated $|S_{11}|$ with stretching along x-axis.

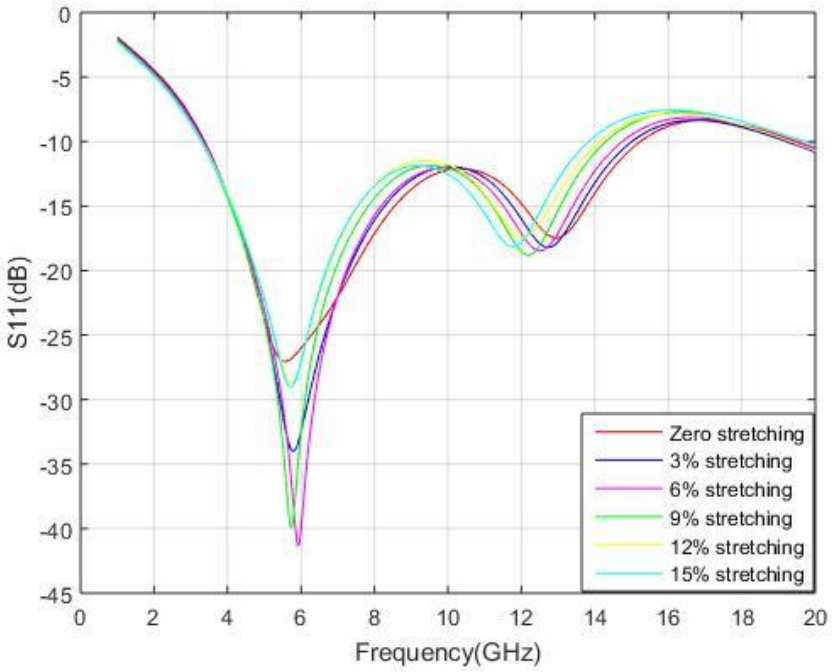

Figure 4.5 Simulated $|S_{11}|$ with stretching along y-axis.

Due to the applied strain, we have a shift at the resonance frequencies and this change is accounted by changing the dimensions of the antenna as a function of the applied strain. PDMS is a typical hyperelastic material and we consider that the total volume is constant during deformation [24]. The length and thickness of the antenna shrink proportionally, when it is stretched along its width and the lower resonance frequency f_{rl} is determined using equation 4.1. When a tensile strain of s is applied along x-axis, the new dimensions of the antenna, width w, length L, thickness h as the function of s are [1]:

$$W = w_0 * (1 + s) \tag{4.2}$$

$$L = \frac{L_0}{\sqrt{1+s}} \tag{4.3}$$

$$h = \frac{h_0}{\sqrt{1+s}} \tag{4.4}$$

When a strain is applied along y-axis, the width and thickness shrink proportionally. As we can see in Figure 4.4 and Figure 4.5, with stretching, the antenna bandwidth was nearly constant for each value of s.

4.2.2 Other antenna parameters

A prototype of the UWB antenna described in previous part has been simulated. The simulated *s* parameters of the final design have been presented, the impedance bandwidth (S_{11} < −10 dB) can cover nearly the whole UWB 3.1–10.6 GHz and finally, with stretching, the bandwidth of the antenna was nearly constant and keep good value (S_{11}< -10 dB) for the wanted frequencies, which means that the designed antenna is suitable for wearable and stretchable applications.

In this section we will present some of other antenna parameters like radiation pattern, gain, and Voltage Standing Wave Ratio (VSWR).

1. Radiation Patterns

The simulated radiation patterns of the proposed UWB antenna at the frequencies of 4.5 GHz and 9 GHz in 3D polar plot are shown in Figures 4.6 (a) and (b).

The radiation pattern for our antenna is nearly omnidirectional for these frequencies. At 4.5 GHz frequency, we have less deviation in the radiation pattern but when the frequency is increased the similarity in the radiation pattern decreases.

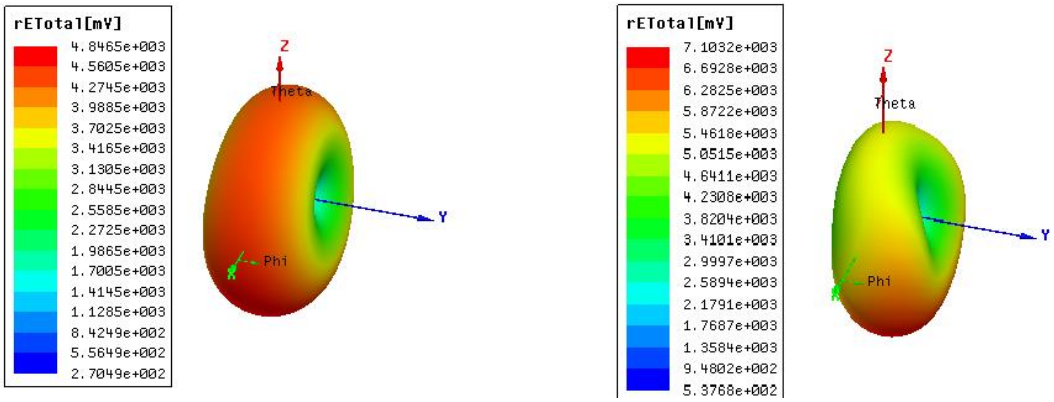

(a) **(b)**

Figure 4.6 3D radiation pattern for the UWB antenna at (**a)** 4.5 GHz (**b)** at 9 GHz.

2. Total Gain

The simulated total gains for the antenna are shown in Figure 4.7

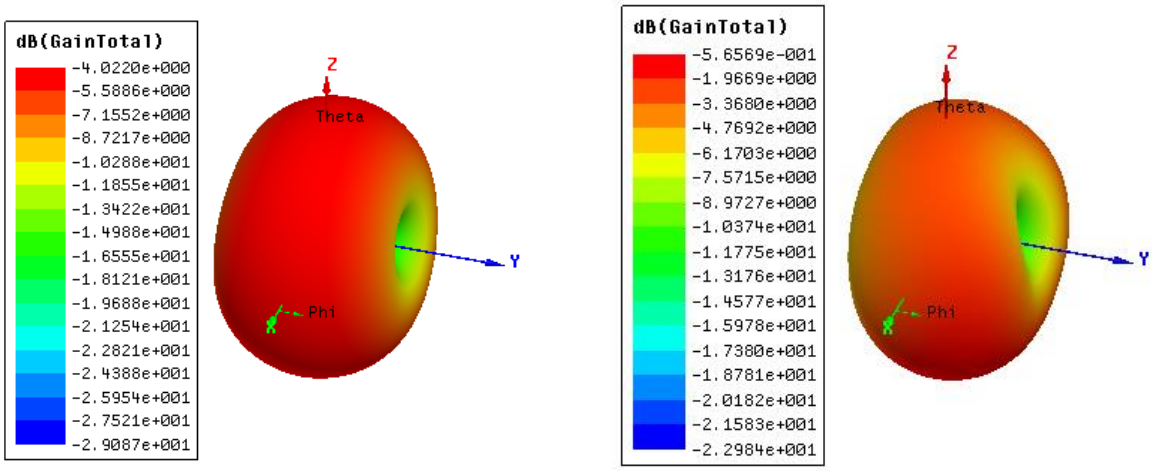

(a) **(b)**

Figure 4.7 3D Gain for the UWB antenna at (**a)** 4.5 GHz **(b)** at 9 GHz.

From these figures, the total gain is omnidirectional at 4.5 GHz and 9 GHz with more deviations at higher frequencies. The gain is small for the UWB antenna.

3. Voltage standing wave ratio VSWR

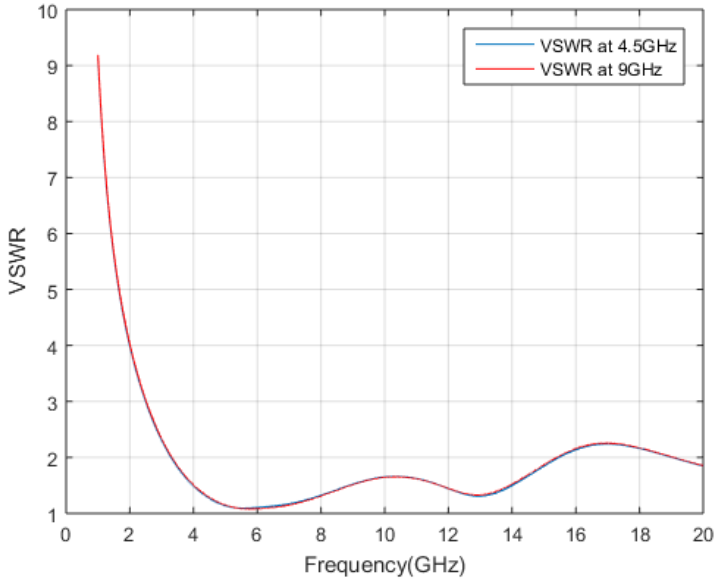

Figure 4.8 VSWR for monopole UWB antenna at 4.5 GHz and 9 GHz.

The VSWR for the UWB antenna shows impedance bandwidth of 3.3 GHz to more than 15 GHz with VSWR < 1.5, which cover nearly the UWB band (3.1-10.6) GHz.

Chapter 5

Design of a MIMO Monopole Patch Antenna for UWB Applications with High Isolation

Chapter Five

Design of a MIMO Monopole Patch Antenna for UWB Applications with High Isolation

Applications such as target detection, radar technology, sensor networks, RFID readers and cellular networks like Long Term Evolution (LTE) need high gains and narrow beamwidths, but the existing UWB antennas have a small gains and omnidirectional radiation pattern [25, 26]. The UWB arrays are good choices for the purpose of achieving good gains and more directive radiation patterns.

The antenna array consists of two, three, or hundreds of antenna elements. The properties of the array and the radiation pattern are affected by some important parameters, mainly, the distance between antenna elements.

Multiple-input multiple-output (MIMO) is a method of using multiple antennas at the transmitter and/or at the receiver to enhance the capacity of the system by deployment the multipath propagation concept. Many systems use the concept of MIMO like LTE, Wi-Fi, and 5G.

5.1 Antenna Design

The other geometry is a compact UWB MIMO antenna shown in Figure 5.1. This antenna was designed with the same material parameters. Two identical patches with dimensions 7 mm X 11 mm were arranged in parallel. Set up more than one antenna elements on the close space, the mutual coupling between them can be very large. The edge-to-edge spacing between the patches is 9 mm which is nearly equal to the half wavelength for the highest frequency (f_{max} = 15 GHz)

which is equal to 20 mm. Each antenna is feed by a 50 Ω microstrip line. The dimensions of the ground plane are w_{gnd} X l_{gnd} mm^2 and for improving the impedance matching at high frequencies, a rectangular slot with dimensions of w_2 X l_2 mm^2 is cut on the ground plane underneath each feeding line. Finally, ground stubs were added on the ground plane of the antenna.

Various techniques have been checked to combine UWB technology with MIMO techniques trying to reduce the mutual coupling between elements and getting a compact size. The proposed structures can efficiently improve isolation and increase the bandwidth across the whole UWB antenna. The optimized dimensions for the substrate of the UWB MIMO antenna are 32 X 18 mm^2 and all other dimensions are the same like the previous antenna.

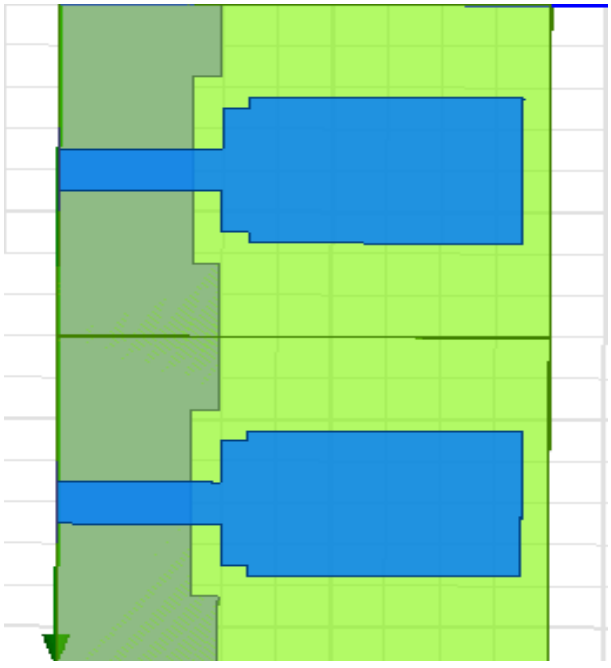

Figure 5.1 The top view of the UWB MIMO antenna.

5.2 Results and Discussion

As shown in Figure 5.1, when placing the two antennas close to each other, the UWB frequency band is covered. Figure 5.2 shows the S-parameters, S_{11} and S_{12}, in dB for the MIMO UWB antenna.

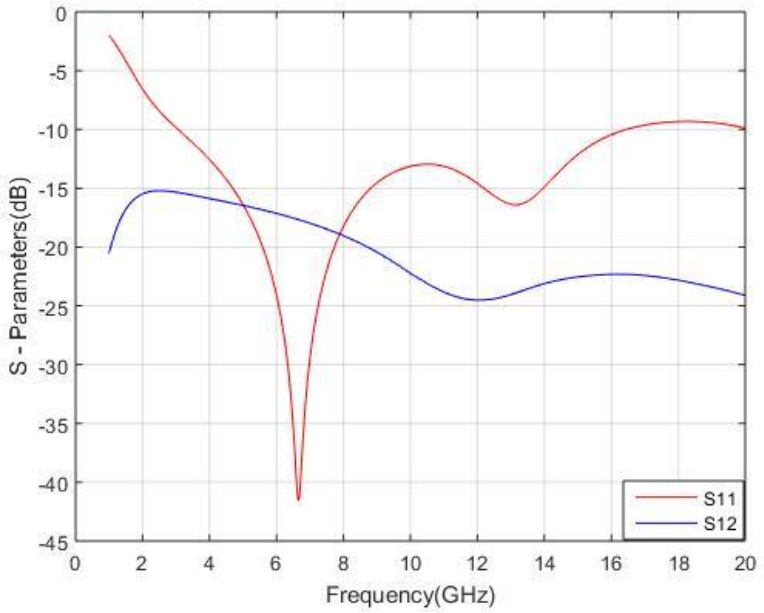

Figure 5.2 S-Parameters for MIMO antenna.

S_{11} is less than -10 dB and S_{12} is less than -15 dB for the desired frequencies, $S_{11}$is acceptable and S_{12} is wanted to be less than -25 dB for UWB applications. So, we need to improve isolation between antenna elements.

5.2.1 Improving Isolation

Mutual coupling between antennas should be minimized in order to maintain high efficiency of the overall system [2]. To reduce it in the UWB band, several structures are applied in the proposed UWB MIMO antenna. These structures achieve high isolation because of different mechanisms. One of them, changing the current distribution in the ground plane using stubs,

which will reduce the mutual coupling by capturing the current towards them. Also, an improvement in the impedance matching will happen.

One of these structures is an AgNWs sheet which was introduced vertically between the radiating elements, between the substrate of each antenna. Using this sheet, the mutual coupling is improved for the band of UWB and the isolation is less than -25 dB for the frequency band of 3.9 – 11.9 GHz, as shown in Figure 5.4. Due to the symmetry of the antenna and as S_{22} and S_{12} are identical to S_{11} and S_{21}, respectively, we have only presented S_{11} and S_{12} .

Initially, we introduced an AgNWs sheet between the substrates and then two slots were created to improve the mutual coupling, each slot has 7 mm length and 0.5 mm of thickness as shown in Figure 5.3 a and b.

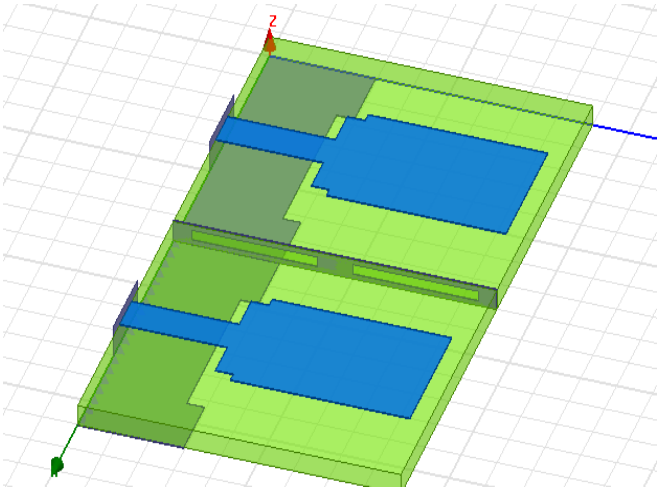

Figure 5.3 (a) Geometries of MIMO antenna with vertical stub.

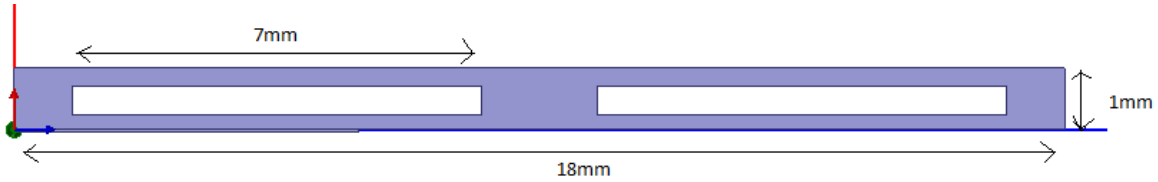

Figure 5.3 (b) Geometries of the stub.

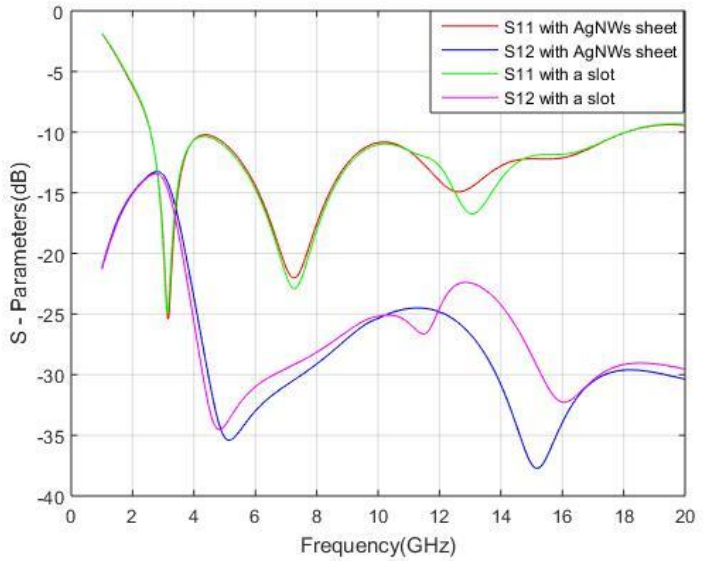

Figure 5.4 S-Parameters for MIMO antenna with vertical stub.

The other structure was a slotted stub in the ground plane as shown in figure 5.5. The mutual coupling for the desired band is improved, and the isolation is less than -25 dB for the frequency band of 3.5-10.6 GHz, as shown in Figure 5.6.

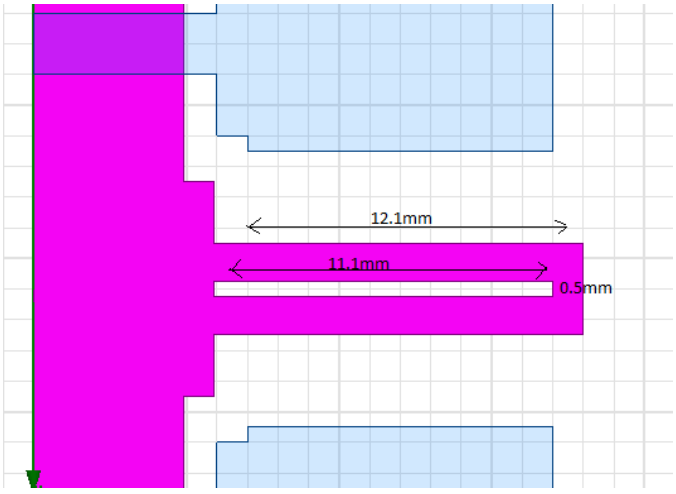

Figure 5.5 Geometries of the ground stub

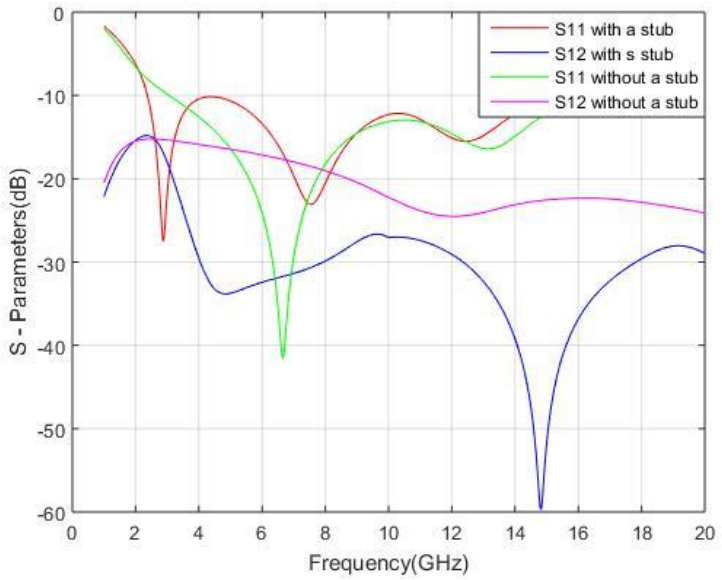

Figure 5.6 S-Parameters for MIMO antenna with and without a ground stub.

Finally, a rectangular loop was added at the end of the ground stub, shown in Figure 5.7. The proposed loop improves the mutual coupling and the isolation is less than -25 dB for the frequency band of 3-10.6 GHz as shown in Figure 5.8.

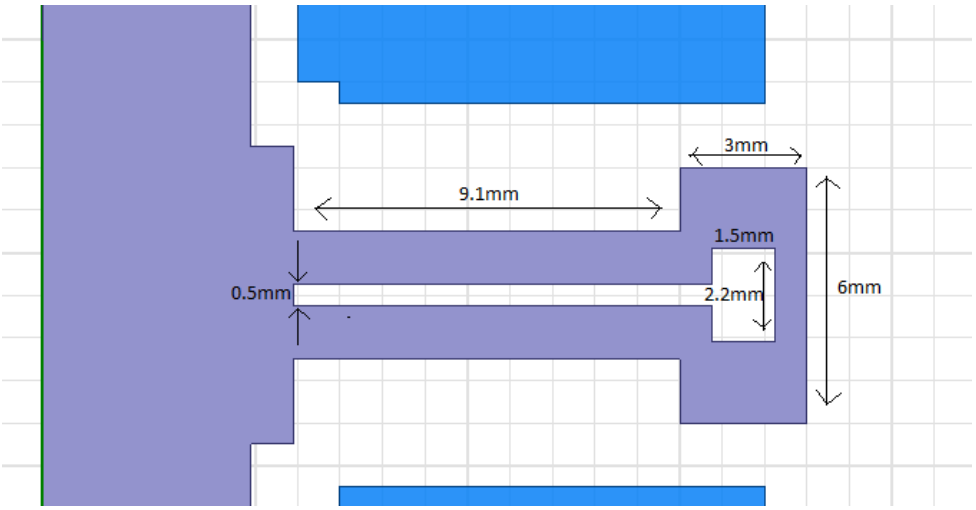

Figure 5.7 Geometries of the ground stub with a loop

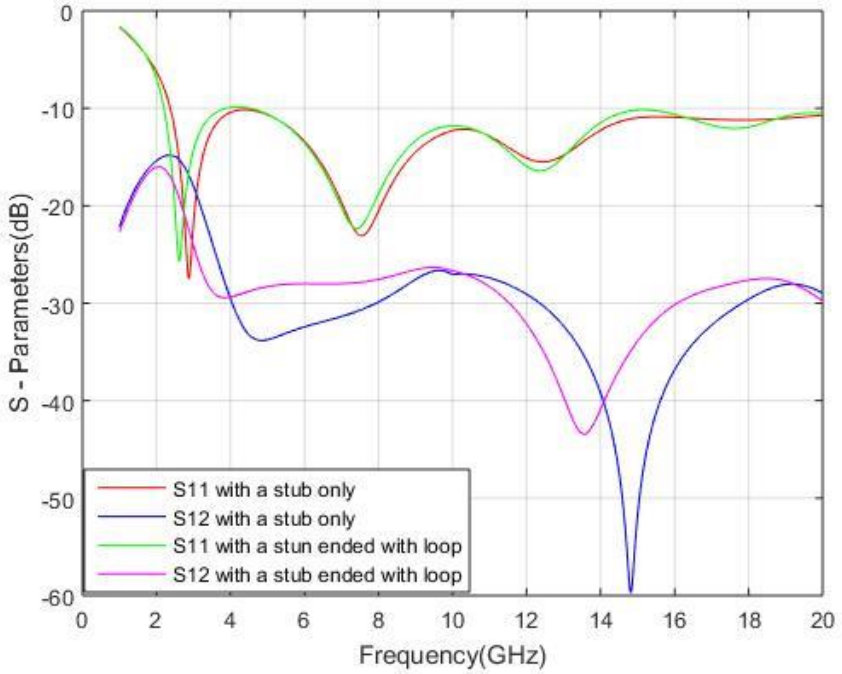

Figure 5.8 S-Parameters for MIMO antenna with and without a rectangular loop.

5.3 Other antenna parameters

In this section we will present other antenna parameters for the previous structures in this chapter like radiation pattern, gain, VSWR, and Current surface distribution.

1. Radiation Patterns

The simulated radiation patterns of the proposed MIMO UWB antenna with and without a vertical loop at the frequencies of 4.5 GHz and 9 GHz in 3D polar plot are shown in Figures 5.9-5.12 (a) and (b).

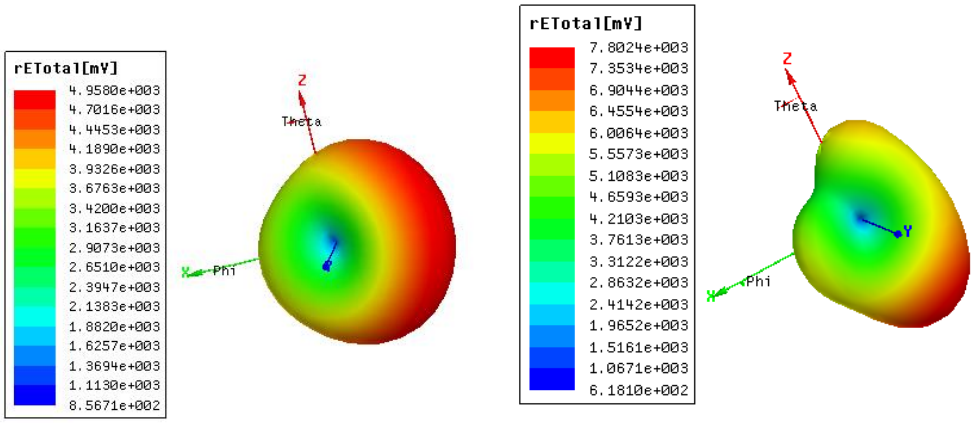

(a) **(b)**

Figure 5.9 3D radiation pattern for the MIMO UWB antenna without any stubs at **(a)** 4.5 GHz **(b)** at 9 GHz

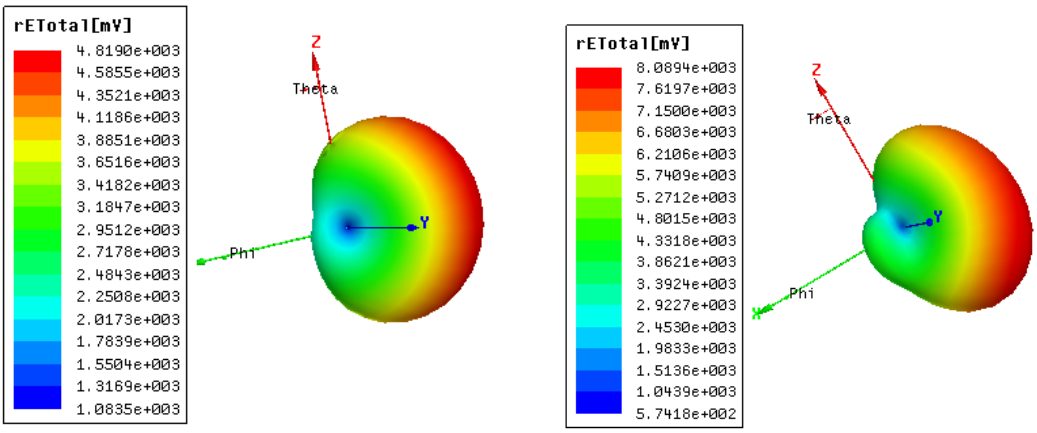

(a) **(b)**

Figure 5.10 3D radiation pattern for the MIMO UWB antenna with a vertical stub at **(a)** 4.5 GHz **(b)** at 9 GHz

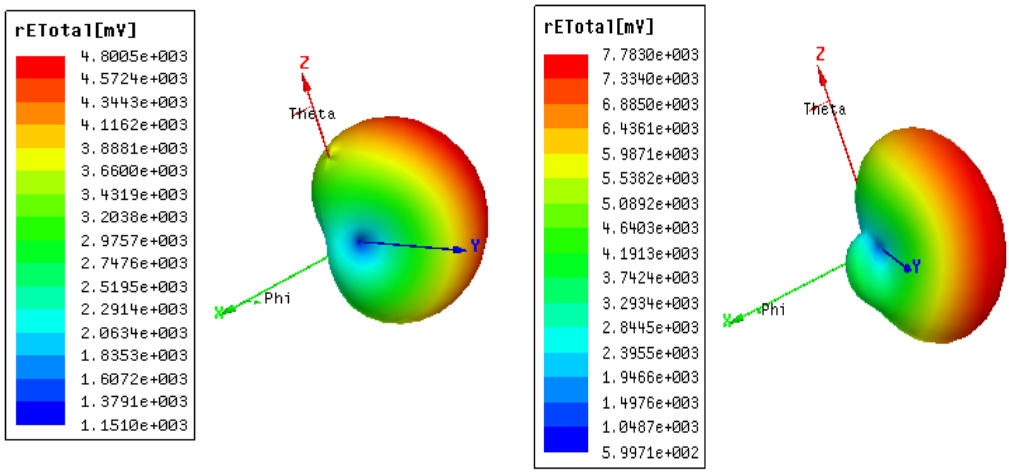

(a) **(b)**

Figure 5.11 3D radiation pattern for the MIMO UWB antenna with a ground stub at **(a)** 4.5 GHz **(b)** at 9 GHz

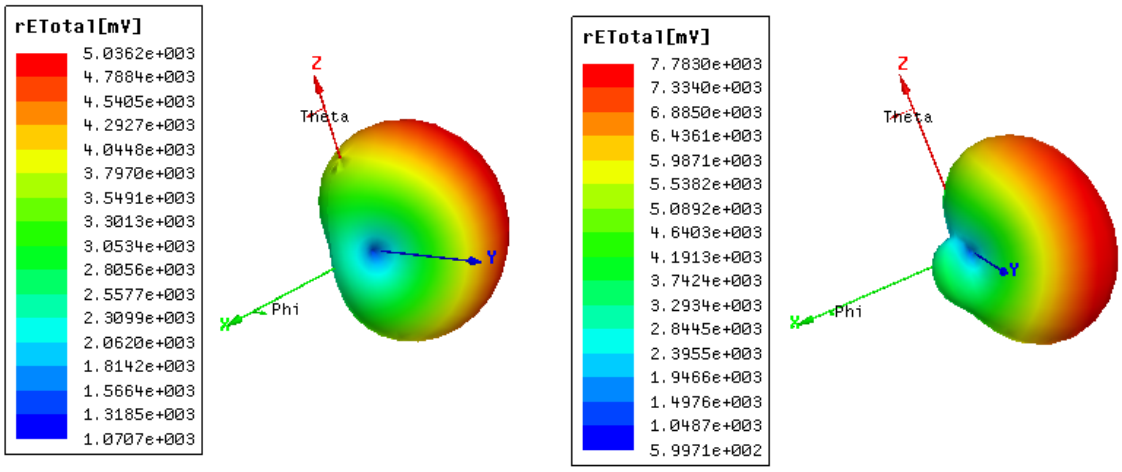

(a) **(b)**

Figure 5.12 3D radiation pattern for the MIMO UWB antenna with a ground stubended with a rectangular loop at **(a)** 4.5 GHz **(b)** at 9 GHz

As we can see, when the MIMO UWB antenna was introduced, the radiation pattern became more directive especially when the stubs were added to the ground plane.

2. Total gain

The simulated total gains for the antenna with different loops are shown in Figure 5.13-5.16.

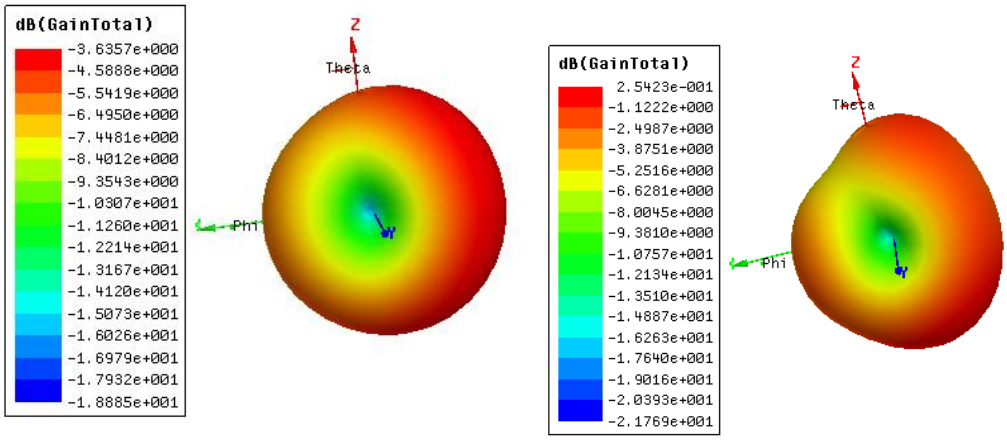

(a) **(b)**

Figure 5.13 3D gain for the MIMO UWB antenna at **(a)** 4.5 GHz **(b)** at 9 GHz

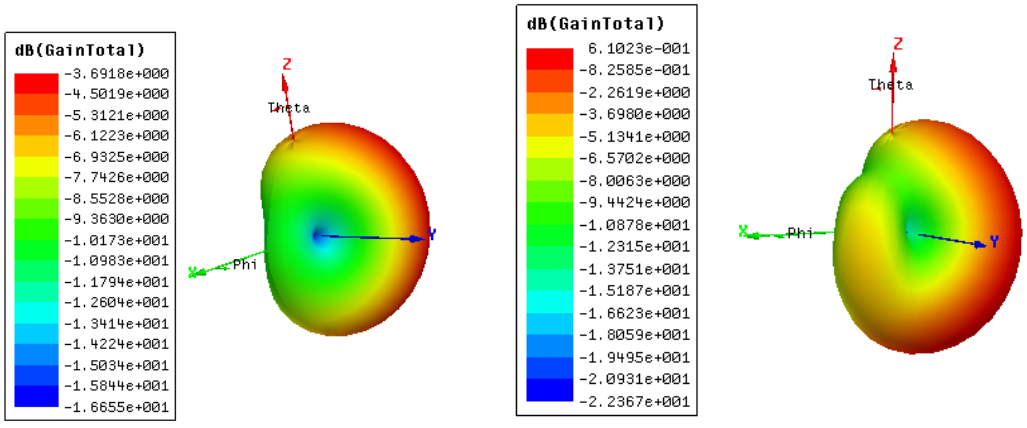

(a) **(b)**

Figure 5.14 3D gain for the MIMO UWB antenna with a vertical stub at **(a)** 4.5 GHz **(b)** at 9 GHz

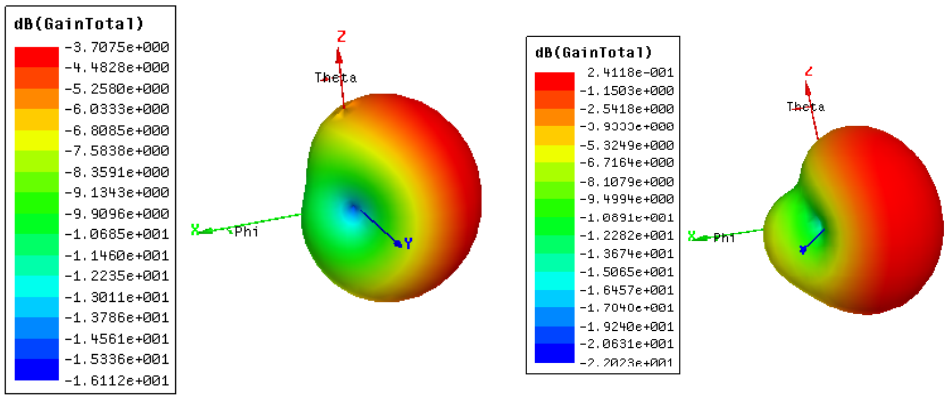

(a) **(b)**

Figure 5.15 3D gain for the MIMO UWB antenna with a ground stub at **(a)** 4.5 GHz **(b)** at 9 GHz

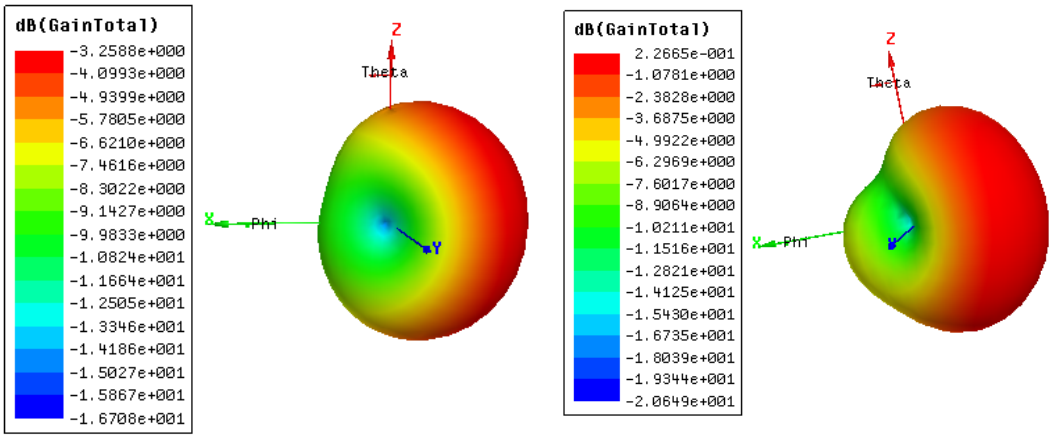

(a) **(b)**

Figure 5.16 3D gain for the MIMO UWB antenna with a ground stub ended with rectangular loop at **(a)** 4.5 GHz **(b)** at 9 GHz

A clear improvement in the total gain was noticed when the MIMO UWB was simulated especially at higher frequencies with vertical stub and the directivity was better at certain direction with these stubs. Before any stub was presented, the total gain was still omnidirectional with more deviations at higher frequencies.

3. Current surface distribution

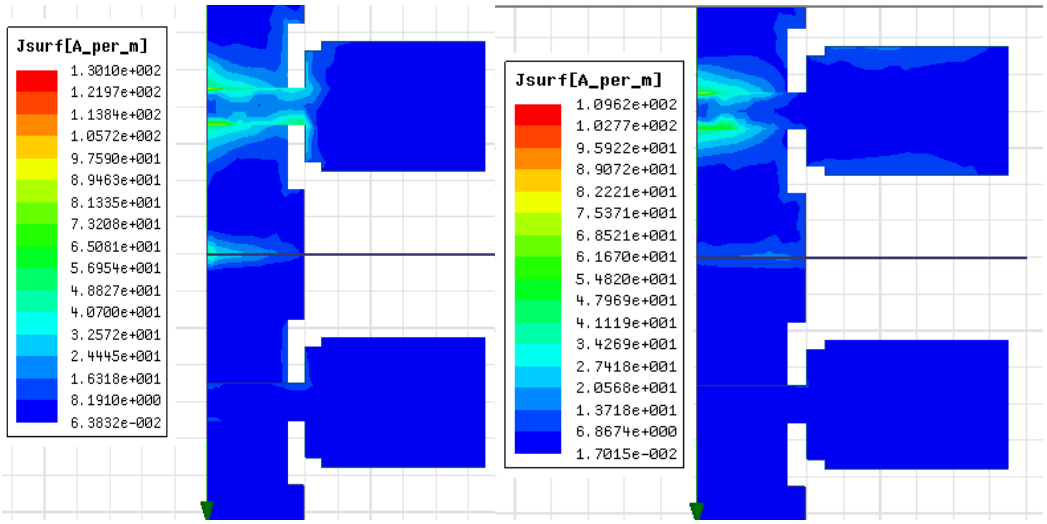

(a) **(b)**

Figure 5.17 The current surface distribution for the MIMO UWB antenna without stubs at **(a)** 4.5 GHz **(b)** at 9 GHz

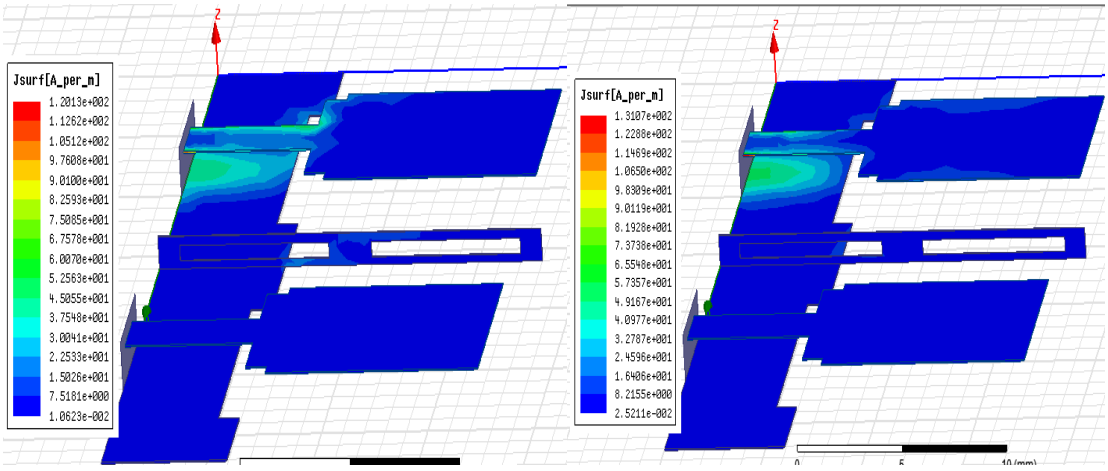

(a) **(b)**

Figure 5.18 The current surface distribution for the MIMO UWB antenna with a vertical stub at (**a)** 4.5 GHz **(b)** at 9 GHz

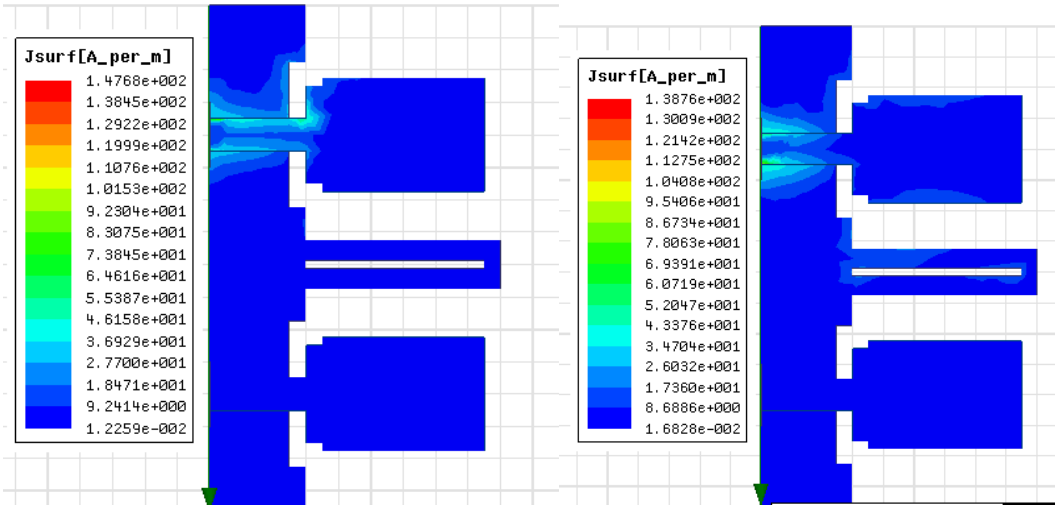

Figure 5.19 The current surface distribution for the MIMO UWB antenna with a ground stub at (**a)** 4.5 GHz **(b)** at 9 GHz

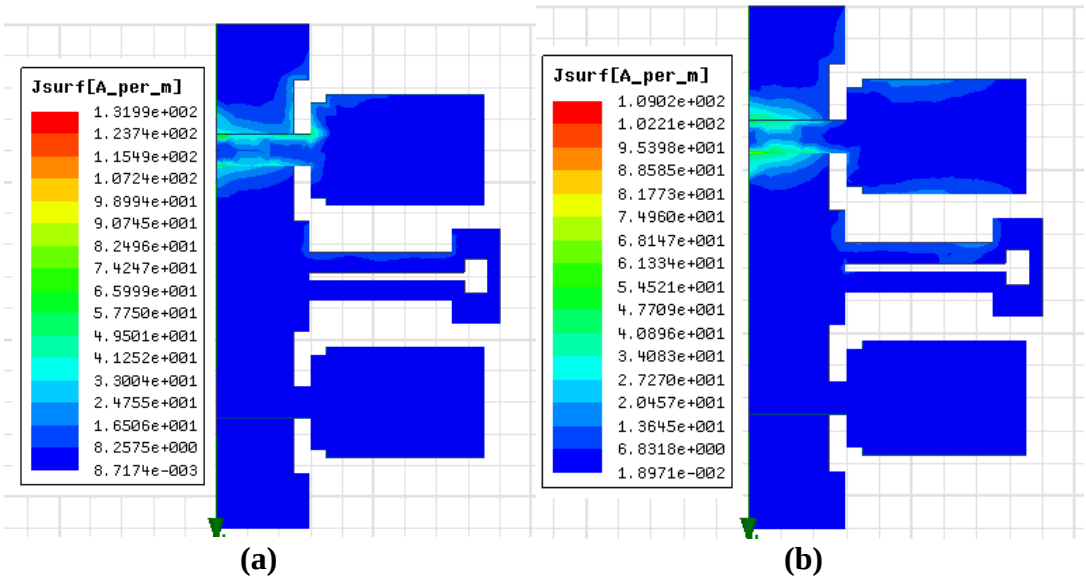

Figure 5.20 The current surface distribution for the MIMO UWB antenna with a ground stub ended with a rectangular loop at (**a)** 4.5 GHz **(b)** at 9 GHz

The ground stubs improved the isolation between two elements by changing the current distribution in the ground plane. The mutual coupling was reduced by capturing the current towards these stubs and an improvement in the impedance matching is occurred.

5.4 Performance Comparison

In this section, a quick comparison will be done between the proposed antenna and recently reported UWB MIMO antenna [2,27,28,29] on the size, isolation and bandwidth. Table 2 shows this comparison. Our antenna achieves good isolation performance with compact size. Therefore, it is a good candidate for UWB MIMO system applications.

Table 2. Performance comparaison of the proposed antenna and some referance antennas.

Reference	Size (mm^3)	Bandwidth (GHz)	Isolation (dB)
2	26 × 31 × 0.78	2.8–12	-25
27	35 × 40 × 0.8	3–11.6	-16
28	27 × 30 × 0.8	3–11	-20
29	22 × 36 × 1.6	3.1–11	-15
Our Work	32 × 18 × 1	3–15	-25

Chapter 6

Conclusion and Future Work

Chapter Six

Conclusion and Future Work

6.1 Conclusion

We have demonstrated a class of monopole UWB antenna that are stretchable and reversibly deformable. An UWB monopole antenna was simulated and the main antenna parameters were analyzed such that S parameter, Voltage Standing Wave Ratio, and radiation properties of the antenna were characterized under stretching along x-axis and y-axis. Also, a tight UWB MIMO antenna was proposed and an isolation improvement was made for an UWB application. This improvement was presented by using different stubs to improve mutual coupling and impedance matching. Based on the simulated performance, the MIMO antenna is good choice for UWB applications.

6.2 Future Work

In order to develop this research, we propose the following ideas as a future work:

1- Increase number of the radiating elements to make additional improvement to the directivity and the gain depending on the applications which will be used for.
2- Increase the number of loops at each UWB MIMO antennas to check its effects on the antenna parameters mainly the isolation.

References

[1] Song, Lingnan, et al. "Stretchable and reversibly deformable radio frequency antennas based on silver nanowires." ACS applied materials & interfaces 6.6 (2014): 4248-4253.

[2] Malekpour, Narges, and Mohammad A. Honarvar. "Design of high-isolation compact MIMO antenna for UWB application." Progress In Electromagnetic Research C 62 (2016): 119-129.

[3] Rappaport, Theodore S. *Wireless communications: principles and practice*. Vol. 2. New Jersey: prentice hall PTR, 1996.

[4] Balanis, Constantine A. *Antenna theory: analysis and design*. John wiley & sons, 2016.

[5] Haykin, Simon S., and Michael Moher. *Modern wireless communications*. Pearson Education India, 2011.

[6] Chang, Dau-Chyrh, and8 Cheng-Nan Hu. "Smart antennas for advanced communication stems." *Proceedings of the IEEE*100.7 (2012): 2233-2249.

[7] Gao, Si-Ping, et al. "Installed Radiation Pattern of Patch Antennas: Prediction based on a novel equivalent model." IEEE Antennas and Propagation Magazine 57.3 (2015): 81-94.

[8] Takshi, Arash, and John D. Madden. "Multilayer stretchable conductors with a large tensile strength." *Journal of Elastomers & Plastics* 42.4 (2010): 365-373.

[9] Nagrial, M. H., and A. Hellany. "Radiated and conducted EMI emissions in switch mode power supplies (SMPS): sources, causes and predictions." Proceedings. IEEE International Multi Topic Conference, 2001. IEEE INMIC 2001. Technology for the 21st Century.. IEEE, 2001.

[10] Peixeiro, Custodio. "Microstrip patch antennas: An historical perspective of the development." *2011 SBMO/IEEE MTT-S International Microwave and Optoelectronics Conference (IMOC 2011)*. IEEE, 2011.

[11] Bisht, Sourabh, et al. "Study the various feeding techniques of microstrip antenna using design and simulation using CST microwave studio." International Journal of Emerging Technology and Advanced Engineering 4.9 (2014).

[12] Rowe, Wayne ST, and Rod B. Waterhouse. "Investigation into the performance of proximity coupled stacked patches." *IEEE transactions on antennas and propagation* 54.6 (2006): 1693-1698.

[13] Kokila, P., T. Saranya, and S. Vanitha. "Analysis and Design of Rectangular Microstrip Patch Antenna Using HFSS." Journal of Network Communications and Emerging Technologies (JNCET) www. jncet. org 6.4 (2016).

[14] Patel, B. D. "Microstrip Patch Ante nna-A Historical Pe rspe ctive of the Developme nt." *Proceedings of the Conference on Advances in Communication and Control Systems-2013*. Atlantis Press, 2013.

[15] Chen, Xiaodong, et al. *Antennas for global navigation satellite systems*. John Wiley & Sons, 2012.

[16] Jan, Jen-Yea, and Liang-Chih Tseng. "Small planar monopole antenna with a shorted parasitic inverted-L wire for wireless communications in the 2.4-, 5.2-, and 5.8-GHz bands." IEEE Transactions on Antennas and Propagation 52.7 (2004): 1903-1905.

[17] Beenamole, K. S. "Microstrip Antenna designs for radar applications." *DRDO Science Sepctrum* (2009): 84-86.

[18] Kim, Dae-Hyeong, et al. "Epidermal electronics." *science*333.6044 (2011): 838-843.

[19] Lipomi, Darren J., et al. "Skin-like pressure and strain sensors based on transparent elastic films of carbon nanotubes." *Nature nanotechnology* 6.12 (2011): 788.

[20] Rai, Tanminder, et al. "A stretchable RF antenna with silver nanowires." *IEEE Electron Device Letters* 34.4 (2013): 544-546.

[21] Aiello, G. Roberto, and Gerald D. Rogerson. "Ultra-wideband wireless systems." *IEEE microwave magazine* 4.2 (2003): 36-47.

[22] Xu, Feng, and Yong Zhu. "Highly conductive and stretchable silver nanowire conductors." *Advanced materials* 24.37 (2012): 5117-5122.

[23] Thomas, K. George, and M. Sreenivasan. "A simple ultrawideband planar rectangular printed antenna with band dispensation." *IEEE Transactions on Antennas and Propagation*58.1 (2010): 27-34.

[24] Xu, Feng, et al. "Strain-release assembly of nanowires on stretchable substrates." *ACS nano* 5.2 (2011): 1556-1563.

[25] Ojaroudi, M., et al. "Small square monopole antenna with enhanced bandwidth by using inverted T-shaped slot and conductor-backed plane." *IEEE Transactions on Antennas and Propagation* 59.2 (2010): 670-674.

[26] Ojaroudi, M., et al. "Small square monopole antenna for UWB applications with variable frequency band-notch function." IEEE Antennas and Wireless Propagation Letters 8 (2009): 1061-1064.

[27] Zhang, Shuai, et al. "Ultrawideband MIMO/diversity antennas with a tree-like structure to enhance wideband isolation." IEEE Antennas and Wireless Propagation Letters 8 (2009): 1279-1282.

[28] Li, Jian-Feng, et al. "Compact dual band-notched UWB MIMO antenna with high isolation." IEEE transactions on antennas and propagation 61.9 (2013): 4759-4766.

[29] Liu, Li, S. W. Cheung, and T. I. Yuk. "Compact MIMO antenna for portable UWB applications with band-notched characteristic." IEEE Transactions on Antennas and Propagation 63.5 (2015): 1917-1924.